12-2023

Investigating Potential Quantitative Trait Loci for Susceptibility to Experimental Autoimmune Encephalomyelitis in the BXD Family of Mice

Margaret Caroline Danehy
University of Tennessee Health Science Center

Investigating Potential Quantitative Trait Loci for Susceptibility to Experimental Autoimmune Encephalomyelitis in the BXD Family of Mice

Abstract

Multiple Sclerosis is an autoimmune inflammatory condition that causes disability, axonal damage in the central nervous system, and eventual paralysis. One of the main risk factors for developing MS is genetics, with recent studies identifying multiple risk alleles associated the major histocompatibility complex. By utilizing the BXD family of mice, we investigated genetic factors that affect a BXD strain's susceptibility to EAE, an inducible disease model for MS. We induced EAE in several BXD mice strains via an emulsion of complete Freund's adjuvant and MOG35-55, and then measured disease severity in each strain. From there, we measured incidence rate of EAE, average peak clinical score, average day of disease onset, average length of acute onset, and average end clinical score. Afterwards, we tested EAE severity in the BXD43 mouse by identifying changes in immune cell populations in the spinal cord, changes in cytokines and chemokines, and distribution of the Fc multimer drug M019. Out of 16 strains tested, we identified 6 BXD strains susceptible to developing EAE, and found suggestive evidence of QTLs on chromosomes 5 and 11. We also found that the BXD43 strain expressed an extreme phenotype, categorized by increased immune cell populations in the spinal cord comparable to the B6 EAE model with pertussis toxin. These results suggest the potential for QTLs to exist on chromosomes 5 and 11, though more BXD strains need to be tested. Additionally, the BXD43 strain shows promise as an extreme phenotype model for EAE, which may serve as an effective model for primary progressive multiple sclerosis.

Document Type

Thesis

Degree Name

Master of Science (MS)

Program

Biomedical Sciences

Research Advisor

Elizabeth A. Fitzpatrick, PhD

Keywords

BXD;EAE;Multiple Sclerosis

Subject Categories

Medicine and Health Sciences

UNIVERSITY OF TENNESSEE HEALTH SCIENCE CENTER

MASTER OF SCIENCE THESIS

Investigating Potential Quantitative Trait Loci for Susceptibility to Experimental Autoimmune Encephalomyelitis in the BXD Family of Mice

Author:
Margaret Caroline Danehy

Advisor:
Elizabeth Fitzpatrick, PhD

A Thesis Presented for The Graduate Studies Council of
The University of Tennessee Health Science Center
in Fulfillment of the Requirements for the Master of Science degree from
The University of Tennessee

in

Biomedical Sciences: Microbiology, Immunology, and Biochemistry
College of Graduate Health Sciences

December 2023

DEDICATION

I would like to dedicate this thesis to several people who have supported and guided me throughout my journey. To my parents, Jennifer and Patrick, who raised and encouraged me to never stop asking questions and searching for answers. To my older sister Katie, a role model and best friend through thick and thin. To my brother-in-law Owen, nephew Parker, and niece Mallie, who's love and joy never fail to make me smile. To my grandfather and grandmother, who are always with me. To my college friends, who helped keep me sane throughout the hardest days. And finally, to my partner, Katie, who's love and belief in my ability never wavered, even on days where I doubted myself. Your love and support have given me so much strength, and it means the world to me that you want to listen to everything I am passionate about. And I look forward to the graduation sword you promised me.

ACKNOWLEDGEMENTS

I'd first like to thank my advisor, Dr. Fitzpatrick, for giving me the opportunity to join her lab and for her dedication to helping me finish my journey through graduate school.

I'd also like to thank my committee members, Dr. Radic and Dr. Yi, for their support in my studies.

Finally, I would like to thank my coworkers, Kellie Brown and Jin Wang, both for their advice for navigating graduate school, as well as their help in both research and data analysis for my studies.

PREFACE

This thesis is organized in a way that first introduces readers to our rationale for choosing the research topic and objectives, as well as an overview of the literature. Next, the materials and methods used are described, which then leads to a presentation of the research. Next, the results of this research are discussed, followed by a concluding chapter to identify the final conclusions of this research and its overall significance.

NOTE ON PDF NAVIGATION: Document navigation is greatly facilitated by using Adobe Acrobat's "Previous view" and "Next view" functions. For "Previous view," use quick keys Alt/Ctrl+Left Arrow on PC or Command+Left Arrow on Mac. For "Next view," use Alt/Ctrl+Right Arrow on PC or Command+Right Arrow on Mac. Using these quick keys in tandem allows the reader to toggle between document locations. Since every scroll represents a new view; depending on how much scrolling is done for a specific view destination, more than one press of the back or forward arrows may be needed. For additional navigational tips, click View at the top of the PDF, then Page Navigation. These Adobe Acrobat functions may not be functional for other PDF readers or for PDFs opened in web browsers.

ABSTRACT

Multiple Sclerosis is an autoimmune inflammatory condition that causes disability, axonal damage in the central nervous system, and eventual paralysis. One of the main risk factors for developing MS is genetics, with recent studies identifying multiple risk alleles associated the major histocompatibility complex. By utilizing the BXD family of mice, we investigated genetic factors that affect a BXD strain's susceptibility to EAE, an inducible disease model for MS. We induced EAE in several BXD mice strains via an emulsion of complete Freund's adjuvant and MOG_{35-55}, and then measured disease severity in each strain. From there, we measured incidence rate of EAE, average peak clinical score, average day of disease onset, average length of acute onset, and average end clinical score. Afterwards, we tested EAE severity in the BXD43 mouse by identifying changes in immune cell populations in the spinal cord, changes in cytokines and chemokines, and distribution of the Fc multimer drug M019. Out of 16 strains tested, we identified 6 BXD strains susceptible to developing EAE, and found suggestive evidence of QTLs on chromosomes 5 and 11. We also found that the BXD43 strain expressed an extreme phenotype, categorized by increased immune cell populations in the spinal cord comparable to the B6 EAE model with pertussis toxin. These results suggest the potential for QTLs to exist on chromosomes 5 and 11, though more BXD strains need to be tested. Additionally, the BXD43 strain shows promise as an extreme phenotype model for EAE, which may serve as an effective model for primary progressive multiple sclerosis.

TABLE OF CONTENTS

LIST OF TABLES

LIST OF FIGURES

LIST OF ABBREVIATIONS

AES	Average end score
APCS	Average peak clinical score
ANOVA	Analysis of Variance
B6	C57BL/6
BBB	blood-brain barrier
BSA	Bovine serum albumin
CC	Chemokine, C-C motif
CD	Cluster of differentiation
CFA	Complete Freund's Adjuvant
CIS	Clinically Isolated Syndrome
CNS	Central nervous system
CSF-1	Colony-stimulating factor 1
CXC	Chemokine, C-X-C motif
D2	DBA2
DMSO	Dimethyl sulfide
DNase	Deoxyribonuclease
DOL	Degree of labeling
DPBS	Dulbecco's phosphate buffered saline
EAE	Experimental autoimmune encephalomyelitis
EBV	Epstein-Barr virus
FACS	Flow Cytometry
Fc	fragment crystallizable region
FCS	Fetal calf serum
GM-CSF	Granulocyte-macrophage colony-stimulating factor
GRO	Growth related oncogene
GWAS	Genome wide association study
IFN	Interferon
IgG	Immunoglobulin G
IL	Interleukin
IP	Interferon gamma induced protein
IR	Incidence rate
IVIG	Intravenous immunoglobulin therapy
IVIS	In vivo imaging spectrum
LRS	Likelihood ratio statistic
Ly	Lymphocyte antigen
MCP	Monocyte chemoattractant protein
MFI	Mean fluorescence intensity
MHC	Major histocompatibility complex
MIP	Macrophage inflammatory protein
MOG	Myelin oligodendrocyte glycoprotein

MS	Multiple Sclerosis
PBS	Phosphate buffered saline
PLP	myelin proteolipid protein
PPMS	Primary-progressive MS
PTX	Pertussis toxin
QTL	Quantitative trait loci
RANTES	Regulated on activation, normal T cell expressed and secreted
RRMS	Relapsing-remitting multiple sclerosis
SPMS	Secondary-progressive MS
TCR	T cell receptor
TNF	Tumor necrosis factor
Tregs	Regulatory T cells
UTHSC	University of Tennessee Health Science Center

CHAPTER 1. INTRODUCTION

Multiple Sclerosis

Multiple Sclerosis (MS) is the world's most common chronic inflammatory disease affecting the central nervous system (CNS) [1]. The disease affects an estimated 2.8 million people worldwide, with incidence rates increasing worldwide [2]. Most individuals are diagnosed at the ages of 20-40 and the disease is twice as common in women than in men. Symptoms of the disease include muscle weakness, tingling, blurred vision, muscle atrophy, vision loss, chronic pain, and eventual paralysis [3]. Patients also show abnormalities in white matter in the brain that form lesions, which in addition to physical symptoms are required for diagnosis [3]. Inflammation in the brain is present throughout all stages of disease, and inflammation is associated with axonal damage and neurodegeneration [4]. Disease progression is slow, with about 50% of patients requiring a wheelchair at around 10-20 years after diagnosis, becoming a significant disabling disease in young adults [5]. Patients typically have a reduced lifespan of 7-14 years [6]. Though MS has been the subject of study for many years, there is no known cure for the disease. Current disease modifying treatments focus on minimizing symptoms and increasing time between relapses.

MS Subtypes

MS is a heterogeneous disease that presents in three main subtypes. Relapsing-remitting MS (RRMS) is characterized by periods of demyelination, neurological dysfunction, and disability, followed by a period of relaxed symptoms, then eventual relapse. These periods of relapse typically increase in severity over time, with many patients eventually developing secondary progressive MS (SPMS). In SPMS, the demyelination and neurological dysfunction begins to decline with no period of remission. Finally, primary progressive MS (PPMS) is characterized by continuous demyelination from the beginning, with no period of remission. About 85% of patients with MS present the RRMS subtype, with only 15% presenting the PPMS subtype [3]. Most available treatments for MS have been found to be effective for treating RRMS, but very few treatments are available for PPMS [7]. This shows a growing need for more treatment options for PPMS.

Pathology of MS

MS is thought to be an autoimmune disease caused by autoreactive T cells that target myelin sheaths on neurons and the cells that produce myelin, oligodendrocytes, in the central nervous system. The resulting demyelination causes axon dysfunction, numbness, pain in the arms and legs, muscle weakness, vision loss, and cognitive impairment, with eventual paralysis. A characteristic diagnostic criterion of MS is demyelination lesions, or areas of the brain with decreased myelination and increased

numbers of inflammatory immune cells. Recent studies have shown that the composition of these lesions may indicate the degree of severity of disease, with larger and more diffuse lesions indicating higher severity of disease symptoms [8]. Disease progression typically starts with invasion of the brain by peripheral inflammatory cells that bypass the blood brain barrier (BBB), as well as activation of proinflammatory microglia. Afterwards, inflammatory B and T cells then follow and cause additional damage to myelin sheaths, resulting in a persistent acquired immune response towards myelin protein [3]. The resulting demyelination causes axonal damage and neurodegeneration, resulting in paralysis and muscle weakness.

Immunopathology of MS

In MS, inflammatory cells from both the innate and the adaptive immune systems will bypass the BBB and begin damaging myelin proteins, particularly T cells. Lesions from MS patients have shown increased levels of T cells and B cells, as well as high levels of demyelination, when compared to nearby healthy white matter [4]. Other studies have shown T_H1 and T_H17 cells play an important role in MS by interacting with circulating inflammatory monocytes that produce cytokines such as IL-6 and IL-12 [9]. As reviewed in Moser, T. et al, 2020, T_H17 cells and elevated levels of IL-17 have been found in both brain samples and spinal fluid samples of MS patients [10]. Additionally, once the circulating monocytes enter the CNS, they can differentiate into inflammatory macrophages that promote the reactivation of T cells into proinflammatory T_H1 and T_H17 cells, causing further damage [9]. The balance between proinflammatory T_H1 cells and regulatory T cells (Tregs) has been found to be skewed in patients with MS, with patients in the relapsing stage of RRMS showing higher levels of T_H1 cells [11]. An increase of Tregs may contribute to the remission phase of RRMS, and the cycling between these two populations may be a primary factor in RRMS [11]. Additionally, other studies have also shown reduced FoxP3 expression in Tregs in patients with PPMS, which is associated with suppressed regulatory function in Tregs [12].

While T cells have historically been the primary focus of MS research, recent studies have also shown the role of other cells such as macrophages, monocytes, and B cells. One study showed a decrease in regulatory macrophages and microglia in white matter samples of MS patients [13]. Another study showed elevated levels of activated monocytes in the peripheral blood of patients with newly diagnosed MS [14]. Finally, as reviewed in Comi, G. et al, 2021, B cells may also play a role in MS development, with treatment of anti-CD20 antibodies proving successful at treating MS [15]. The interaction of all these different immune cells seem to contribute to the development of MS.

Risk Factors

There are several risk factors that affect an individual's susceptibility to MS. One major risk factor is smoking, though it has only been found to be smoking tobacco that increases risk, rather than use of oral tobacco [16]. This suggests that it is the

inflammation and irritation of smoking, rather than nicotine itself, that increases the risk for MS development. Additionally, active smoking can also increase the rate of relapses and disease severity in individuals with RRMS [17]. Another risk factor is low vitamin D levels, which may be associated with the increase in MS prevalence in areas further from the equator, where people are exposed to less sunlight [18]. As reviewed in Miclea, A et al, 2020, vitamin D has an immunoregulatory effect by promoting anti-inflammatory responses and apoptosis in T cells, B cells, and dendritic cells (DCs) [19]. Another risk factor is biological sex, with women being twice as likely to develop RRMS as men, though it is currently unknown why [18]. Finally, one other major risk factor is prior infection with the Epstein-Barr virus (EBV). One study of over 10 million US service members showed that prior infection with EBV increased the risk of developing MS by almost 32-fold [20]. As reviewed in Soldan, S. S. et al, 2023, it is theorized that EBV proteins may mimic self-antigens, and therefore cause the immune system to begin to target self-antigens in the CNS [21].

Genetics of MS

Genetics also play a substantial role in determining risk for developing MS. About 20% of individuals with MS also have a relative with MS, and twins have been found to have a 25-30% increased risk of developing MS if the other twin has it [18]. Several genomic wide association studies (GWAS) have identified several quantitative trait loci (QTLs) associated with the major histocompatibility complex (MHC) [22]. Further studies have identified that the HLA-DBR1*1501 variant has been associated with MS development in several different patient populations [23]. More recent GWAS studies have expanded the list of associated HLA loci [24]. One GWAS formulated a genetic map that linked a few hundred genes to MS, with 32 associations focused on the major histocompatibility complex. This study also found that the following cell populations have the highest number of genes associated with MS susceptibility: B cells, T cells, natural killer (NK) cells, myeloid cells, and microglial cells [25, 26]. Taken together, these studies show that the greatest genetic risk factors for MS all involve dysregulation of the MHC, and through that dysregulation of antigen recognition, correlating with the autoimmune pathology of MS.

Treatment Options for MS

While there is no known cure for MS, several disease modifying therapies have been successful at treating MS symptoms and prolonging the time between relapses for RRMS. Of the 15 FDA-approved treatments for RRMS, most focus on promoting anti-inflammatory responses during the relapsing phase, which can reduce MS lesion development and sometimes improve mobility [27]. The first approved treatments for MS include interferons and glatiramer acetate [7]. IFN-β has been shown to increase anti-inflammatory cytokines, as well as help reduce trafficking of immune cells across the BBB [28] Recent studies have shown that treatment with IFN-β can result in an increased expression of regulatory T cells (Tregs), which play a role in maintaining and preventing

autoimmunity [29] As reviewed in Kasindi et al, 2020, glatiramer acetate promotes the transition of helper T cells from the inflammatory T_H1 phenotype to the regulatory T_H2 phenotype [30]. Glatiramer acetate has also been shown to decrease B cell activation. [31]. Other treatment options include monoclonal antibody therapies such as natalizumab, which also helps to prevent migration of inflammatory cells across the BBB [32]. Other monoclonal antibodies include anti-CD20 therapies such as ocrelizumab and ofatumumab that both reduce B cell populations in the patient [32]. However, as with many immunotherapeutic treatments, these treatments often result in compromised immune systems for the patient. Additionally, ocrelizumab is currently the only FDA-approved treatment for PPMS [33]. With only one approved therapy, there is a very clear need for more treatment options for PPMS.

Experimental Autoimmune Encephalomyelitis

The most used animal model for MS research is experimental autoimmune encephalomyelitis (EAE). There are two methods of inducing EAE, referred to as the passive model and the adoptive transfer model. In the passive model, mice are immunized with a subcutaneous injection of an emulsion of a myelin protein and Complete Freund's Adjuvant (CFA). Depending on the protein and mouse strain used, it is sometimes followed by an injection of pertussis toxin (PTX). This PTX injection improves the incidence rate of developing EAE by promoting degradation of the BBB [34]. This immunization produces an autoimmune response to the myelin protein, resulting in demyelination that is caused by autoreactive T cells attacking the myelin sheath, mirroring the pathology of MS [35]. In this model, different mouse strains will react to some myelin proteins and will not react to others. For example, the C57BL/6 (B6) mouse will develop EAE when induced with myelin oligodendrocyte glycoprotein (MOG), while the SJL mouse model will develop EAE when immunized with myelin proteolipid protein (PLP) [36]. The second model, the adoptive transfer model, is used to investigate the role of $CD4^+$ T cells in EAE pathology. In this model, $CD4^+$ T cells are taken from a mouse that has been induced via the passive model, then transferred to a naïve mouse. As the $CD4^+$ T cells are already specific to myelin protein, the new cells begin an autoimmune response to myelin protein, which develops into EAE. Both models have been used to identify different components of the immune system that contribute to the development of EAE.

Innate Immune Response in EAE

Innate immune cells play a vital role in the development of EAE. Both circulating and CNS myeloid cells promote inflammation and neurodegeneration in the CNS, resulting in demyelinating lesions. Microglia and macrophages in the CNS can cycle between a more proinflammatory phenotype to a more regulatory phenotype, though the cells typically express traits of both *in vivo* [37]. During EAE, more microglia and macrophages express proinflammatory traits, and some research has suggested that promotion of the regulatory phenotype may reduce inflammation and neurodegeneration,

[37]. Other cells such as DCs serve as antigen presenting cells (APCs) for inflammatory T cells that migrate into the CNS, promoting more neurodegeneration [38] Finally, neutrophils also play a key role in EAE. As reviewed in Pierson, E. R. et al, 2018, neutrophils promote migration of inflammatory cells to the CNS via production of proinflammatory cytokines such as TNF-α, IFN-γ, IL-6, IL-1β, and IL-12, which promote the maturation of APCs that interact with infiltrating T cells [39]. Additionally, other studies have shown that neutrophils may contribute to the degradation of the blood brain barrier (BBB) during the initial stages of EAE, and that depleting neutrophil activity prevents this degradation [40].

The interaction of several innate immune cell receptors also has a significant impact on EAE development. Some studies have shown how blocking expression of CX_3CR1, the receptor for fractalkine (CX_3CL1), prevents migration of monocytes, macrophages, and DCs into the CNS, thus alleviating EAE symptoms and preventing disease development [41] Another study demonstrated that blocking colony-stimulating factor 1 (CSF-1) in mice with EAE reduced inflammatory myeloid cell activity in the CNS and reduced lesion size, without also depleting regulatory microglia that promote homeostasis [42]. However, the role of certain immune receptors such as CX_3CR1 in EAE has been found to be somewhat contradictory, as other studies have shown that mice that are deficient in CX_3CR1 are also more susceptible to severe EAE. This suggests the receptor may also play a regulatory role by managing antigen-presenting cell activity [43]. Another important receptor is CCR2, a receptor on monocytes for migration [44]. Studies have shown that blocking of CCR2 prevents EAE disease development, while mice with EAE have been shown to have elevated CCR2 expression in the spinal cord [45, 44].

Role of T Cells in EAE

Using the adoptive transfer model, researchers have found that T cells are the primary cell that drives EAE pathogenesis. Further studies have also shown that increased levels of T_H1 and T_H17 cells in mice lead to more severe EAE symptoms and progression in mice in both models of EAE [46]. Migration of autoreactive $CD4^+$ T cells is a key step in the development of EAE. Blocking migration of $CD4^+$ T cells into the CNS has been shown to reduce EAE severity, as the $CD4^+$ T cells are responsible for recruiting other inflammatory cells to the CNS [47] Several studies have also identified a higher expression of T_H17 cells in EAE lesions in the spinal cord, as well as higher concentrations of the proinflammatory cytokine IL-17, which then activates production of other proinflammatory cytokines such as IL-1β [48, 49]. Other studies have looked at the role of regulatory T cells (Tregs) in preventing EAE. Mice with lower levels of Tregs show more severe EAE symptoms, suggesting these cells may have a protective effect by managing autoreactive T cells [50]. Tregs also play a role in maintaining homeostasis in the immune system by suppressing autoimmunity, while dysregulation of Tregs exacerbated autoimmunity. One study found that mice with EAE and suppressed Treg levels showed more severe EAE symptoms, while mice treated with mesenchymal stem cells produced higher numbers of Treg cells and showed reduced EAE severity [51].

Another study showed that dysregulation of Tregs caused by mitochondrial oxidative stress can result in autoimmunity, but if reversed can reduce EAE severity [52]. These various T cell populations all contribute to the development of immune dysregulation and the development of EAE, whether through promoting autoimmune damage to the CNS, or by maintaining homeostasis to prevent disease progression.

EAE Presents Differently in Various Mice Strains

Interestingly, the presentation of EAE differs between mouse strains and myelin proteins used in the immunization [53]. Some mice strains respond better to one myelin protein over another. One study found that the B6 strain can present as either relapsing remitting EAE or chronic EAE by increasing the concentration of myelin oligodendrocyte glycoprotein (MOG_{35-55}) in the CFA/MOG_{35-55} emulsion [54]. By studying different combinations of mouse strains and antigen, EAE can reflect the different subtypes of MS and may offer insight into mechanisms of disease. Notably, most of the current treatments for MS are only applicable to patients with the RRMS subtype, with few treatment options available for patients with PPMS. This highlights the need for more EAE models that can better reflect a wider range of MS subtypes.

Research Objectives

My project had two objectives. For the first objective, I wanted to test EAE induction in the BXD family of mice strains to determine possible QTLs related to EAE susceptibility. To accomplish this, I tested the parent strains B6 and DBA2 (D2) for their susceptibility to EAE using the passive model of EAE. The mice were immunized with CFA/MOG_{35-55} and their weights and clinical scores were recorded from day 7 to day 30. Afterwards, I tested 16 different BXD strains for susceptibility to EAE using the same passive model. Their weights and scores were also measured from day 7 to day 30. Using the data from these studies, the following traits were measured and the results were entered into GeneNetwork: incidence rate of EAE, average peak clinical score, average day of onset, average length of acute onset, and average end score. These results may help us determine new quantitative trait loci (QTL) associated with EAE susceptibility.

For the second objective, I wanted to compare the severe EAE seen in the BXD43 strain to the B6 strain. I first immunized both BXD43 and B6 mice with CFA/MOG and monitored the weights and scores of the mice from day 7 to day 29. I then harvested spinal cords and serum samples from the induced mice at several time points. I analyzed the myeloid cells, microglia, and lymphocytes of the spinal cord samples using flow cytometry. I also measured various inflammatory cytokine and chemokine levels in the serum samples. These results may help establish the BXD43 strain as a potential model for PPMS due to its extreme phenotype of severe EAE.

CHAPTER 2. MATERIALS AND METHODS

Mice and Welfare

Female C57BL/6 (B6) and DBA/2J (D2) mice were obtained from Jackson Laboratories (Bar Harbor, ME). Female BXD mice were obtained from Dr. Robert Williams, University of Tennessee Health Science Center (Memphis, TN). Mice were housed in groups of up to 5 mice in 500 cm^2 solid bottom clear polysulfone plastic cages. Mice were housed in the Trimetis Facility UTHSC Lab Animal Care Unit at biosafety level 2. Mice were kept on a 12-hour light/dark cycle and were fed Irradiated LM-485 Mouse/Rat Diet (19% protein) and acclimated at least 7 days prior to induction.

BXD43 Breeding Colony

A breeding colony was set up for the BXD43 strain. 4 trios of breeders (2 female, 1 male) were grouped together with their respective partners for 2 weeks, then the females were placed in separate cages. The females were then observed for about a month for any possible litters or pregnancy. Once pups were born, litters were weaned after 21 days. Females were separated and were used in future studies, while males were only saved to replace male breeders, otherwise they were sacked. If a litter only had a single female pup, she was kept with the mother for an additional week or combined with another litter of the same age. If the pups were small at weaning, they were also given a supplementary feed cup of DietGel 76A.

EAE Emulsion Preparation

To induce EAE in the mice, an emulsion of CFA/MOG_{35-55} was created. First, 100 mg of desiccated M. Tuberculosis H37 Ra was dissolved in 20 mL of incomplete Freund's adjuvant (**Table 2-1**). The solution was homogenized for 3 minutes using the gentleMACS™ Tissue Dissociator (Miltenyi Biotec, Bergisch Gladbach, Germany), then incubated on ice for 5 minutes. Homogenization and incubation were repeated two more times, resulting in complete Freund's adjuvant (CFA). A 1:10 dilution of the MOG_{35-55} stock solution was made in DPBS, creating a MOG_{35-55} solution at 1 mg/mL. Equal volumes of both CFA and MOG_{35-55} solution were drawn into appropriate syringes, then connected to a 3-way stopcock. The two solutions were then emulsified to create a CFA/MOG_{35-55} emulsion at 0.5 mg/mL of MOG_{35-55}. The emulsion was tested prior to injection by testing a drop of emulsion in water until the drop maintains structure in the water and does not disperse.

Table 2-1. Reagents and kits.

Product	Catalogue Number	Company
Irradiated LM-485 Mouse/Rat Diet	7912	Teklad/Inōtiv (West Lafayette, IN)
M. Tuberculosis H37 Ra	231141	BD Biosciences (Franklin Lakes, NJ)
Incomplete Freund's Adjuvant	263910	BD Biosciences
Myelin Oligodendrocyte Glycoprotein (MOG_{35-55}) protein	HYP1038A	MedChem Express (Monmouth Junction, NJ)
3-way Stopcock w/ Swivel Male Luer Lock	MX5311L	Smiths Medical (Minneapolis, MA)
Dulbecco's Phosphate-Buffered Saline (without calcium and magnesium)	21-031-CV	Corning (Corning, NY)
Cryogenic Vial 5mL	10-500-27	Fisher Scientific (Waltham, MA)
Red Blood Cell Lysing Buffer Hybri-Max	R7757	Sigma Life Science/Sigma-Aldrich (Burlington, MA)
RPM1-1640 (Without L-Glutamine)	12-167F	Lonza™ BioWhittaker (Basel, Switzerland)
Fetal Bovine Serum, Qualified	F6178	Sigma-Aldrich
Penicillin Streptomycin Glutamine (Pen-strep)	10378-016	Gibco (Billings, MT)
2-Mercaptoethanol	60-24-2	Fisher Scientific
Dimethyl Sulfoxide	67-68-5	Fisher Scientific
M019		Gliknik (Baltimore, MD)
FcBlock	553142	BD Biosciences
Deoxyribonuclease (DNase)	DN25	Sigma-Aldrich
Collagenase D	11088858001	Roche Diagnostics GmbH (Mannheim, Germany)
Percoll	P4937	Sigma-Aldrich
Pertussis Toxin (PTX) in glycerol	BT-0105	Hooke Laboratories, Lawrence, MA
Falcon Tissue Culture Flask	353109	BD Biosciences
Serum Separator Tubes	365967	BD Biosciences
ProcartaPlex™ Mouse Cytokine & Chemokine Convenience Panel 1 26-Plex	EPXR360-26092-901).	Invitrogen (Waltham, MA)
CF® Dye & Biotin SE Protein Labeling Kits	92220	Biotium (Fremont, CA)
Phosphate Buffered Saline	10010-023	Gibco
Dylight488 Conjugation Kit (Fast) Lightning-Link	Ab201799	Abcam (Cambridge, United Kingdom)
DietGel 76A	72-07-5022	Clear H_2O (Portland, ME)
UltraComp eBeads- Compensation beads	01-2222-42	Invitrogen

EAE Induction and Observation

Mice were subcutaneously injected with 200µL of CFA/ MOG_{35-55} emulsion. In some studies, one group of mice were also dosed with 110 ng/mouse of pertussis toxin (PTX) 1 hour after induction, and another dose 24 hours after induction. Mice were monitored 24 hours after induction to ensure mice are alert and ambulatory. Mice were observed and weighed daily from day 7-30 post induction, and daily weight percent change was calculated. Mice were scored on a scale of 0-5 for severity of EAE (**Table 2-2**), and the weights and scores were plotted using GraphPad Prism 9 (Dotmatics, Boston, MA). The following BXD strains were tested for susceptibility to EAE: BXD77, BXD79, BXD44, BXD87, BXD48a, BXD73b, BXD89, BXD43, BXD68, BXD125, BXD90, BXD11, BXD213, BXD170, BXD75, and BXD55, as well as the parent B6 and D2 strains.

EAE Spinal Cord Flow Analysis

Spinal Cord Harvest

Mice were harvested on day 15 for the BXD43 mice, day 17 for B6 mice dosed with PTX, and day 29 for B6 with no PTX. On the day of average peak score, mice were euthanized via isoflurane and harvested for serum, spinal cord, brain, and lymph nodes. Serum was collected via blood collection from a cardiac stick, then blood was transferred to serum-separator tubes, and serum was stored in the -80˚C freezer. Brain and lymph nodes were harvested, then placed in cryogenic vials and frozen in dry ice. The samples were then stored in the -80˚C freezer. Spinal cords were transported back to our lab in 10% FCS cell media. Spinal cords were then homogenized in 10mL 10% FCS cell media, 50µL DNase at 1mg/mL and 10µL collagenase at 100mg/mL. The samples were then incubated for 30 minutes in the 37˚C incubator. Samples were then washed with cell media, then filtered through a 40µL filter. Cells were then washed in cell media again, then resuspended in 6mL of 37% percoll. Samples were then spun for 20 minutes at 860 x g. Samples were decanted to remove myelin and washed in cell media.

Spinal Cord Flow Cytometry

Samples were then split into three equal volumes to stain for three panels. The cells were first stained with 2µL of FcBlock, then incubated for 10 minutes at room temperature in the dark. Next, the cells were washed with FACS (flow cytometry) buffer (**Table 2-3**). The cells were then stained with a master mix of fluorescent antibodies (**Table 2-4**) for microglia cells, myeloid cells, and lymphocytes. The cells were then incubated at 4°C in the dark for 30 minutes. The cells were then washed twice, decanted, then 100µL of FACS buffer was added to each sample, bringing the final volume to around 200µL. The cells were then vortexed and plated.

Table 2-2. EAE scoring criteria.

Score	Symptoms
0	No Symptoms
0.5	Tip of tail is limp
1.0	Whole tail limp, cannot wrap around finger to stabilize mouse
1.5	Limp tail and wobbly walk, one leg falls consistently through a wire rack
2.0	Limp tail and wobbly walk, one foot dragging
2.5	Limp tail and both feet show signs of dragging when walking
3.0	Limp tail and complete hind limb paralysis
3.5	Limp tail, complete hind limb paralysis, and mouse cannot orient itself when placed on its back
4.0	Limp tail, complete hind limb paralysis, and minimal movement in cage but mouse is alert
4.5	Limp tail, hind limb paralysis, mouse is not moving or alert
5.0	Mouse is rolling in cage or mouse found dead
Euthanasia Criteria	a) Mouse has a score of 4.0 for longer than 48 hours b) Mouse has a score of 4.5 or 5 c) Mouse loses greater than 30% of total body weight

Table 2-3. FACS buffer components.

Product	Catalogue Number	Company
Bovine Serum Albumin	10735078001	Sigma-Aldrich
Phosphate Buffered Saline	10010-023	Gibco
Magnesium Chloride ($MgCl_2$)	M2670-100G	Sigma-Aldrich
Deoxyribonuclease (DNase)	DN25	Sigma-Aldrich

Table 2-4. Flow cytometry antibodies.

Name and Fluor	Clone	Catalogue Number	Company
Anti-CD11b-APC-Fire	M1/70	101262	BioLegend (San Diego, CA)
Anti-CD19-APC	1D3	550992	BD Pharmagin/BD Biosciences
Anti-Ly6C-PE	HK1.4	128008	BioLegend
Anti-Ly6G-BV605	1A8	127639	BioLegend
Anti-CD115-BV421	AFS98	1355131	BioLegend
Anti-CD206-APC	C068C2	141707	BioLegend
Anti-CD45-BV421	30-F11	103133	BioLegend
Anti-SiglecH-PE	551	129605	BioLegend
Anti-CX3CR1-BV605	SA011f11	149027	BioLegend
Anti-F4/80-AF488	BM8	123120	BioLegend
Anti-IA-IE-APC	M5/114.15.2	107613	BioLegend
Anti-CD80-PE	16-10A1	12-0801-81	BioLegend
Anti-CD11c-BV605	HL3	563057	BD Biosciences
Anti-Ly6C-AF488	HK1.4	128021	BioLegend
Anti-CD8-APC-Fire	53-6.7	100765	BioLegend
Anti-TCRβ-BV605	H57-597	562840	BD Biosciences
Anti-CD69-BV421	H1.2F3	104527	BioLegend
Anti-CD19-PE	eBio1D3	12-0193-82	BioLegend
Anti-CD4-APC	RM4-5	561091	BD Pharmagin
Anti-CD11b-AF488	M1/70	101217	BioLegend

Additionally, the same antibodies were used to prepare single color controls. 1.5 µL of each antibody was added to one drop (around 100µL) of compensation beads, which were then incubated for 30 minutes at 4°C in the dark. The beads were then washed twice with FACS buffer, decanted, then 100µL of FACS buffer was added to bring the final volume to about 200µL. The beads were then vortexed and plated.

As shown in **Table 2-5**, the samples were then stained with several fluorescent antibodies specific to the desired cell markers. The first panel for microglial cells contained the following antibodies: Anti-CD11b-APC-Fire, Anti-CD206-APC, Anti-CD45-BV421, Anti-SiglecH-PE, Anti- CX3CR1-BV605, and Anti-F4/80-AF488. The second panel for myeloid cells contained the following antibodies: Anti-CD11b-APC-Fire, Anti-IA-IE-APC, Anti-CD45-BV421, Anti-CD80-PE, Anti-CD11c-BV605, and Anti-Ly6C-AF488. The third panel for lymphocytes contained the following antibodies: Anti-CD8-APC-Fire, Anti-TCRβ-BV605, Anti-CD69-BV421, Anti-CD19-PE, and Anti-CD4-APC. Samples were then analyzed using the Bio-Rad ZE5 Cell Analyzer (Bio-Rad, Hercules, CA). The data was then analyzed, and cell percentages were measured using FlowJo (BD Biosciences, Franklin Lakes, NJ). Significance between the BXD43 samples and the B6 samples was calculated in GraphPad Prism 9 (Dotmatics, Boston, MA) using a one-way ANOVA followed by Tukey's post comparison test to compare mean of each group to all other groups. A value of $p < 0.05$ was considered significant.

Serum Cytokine and Chemokine Multiplex Immunoassay

Serum Collection

Serum samples were collected from female C57BL/6 and BXD43 mice. Mice were euthanized with isoflurane and a cardiac stick was performed to collect whole blood. The blood samples were then transferred to serum-separator tubes, and serum aliquoted into 55µL samples, then stored in the -80˚C freezer. Samples were then thawed and ran through a cytokine and chemokine detection kit. 50µL of capture beads were added to each sample well, and liquid was removed. 25µL of Universal Assay Buffer was added to each well, and afterwards 25µL of serum sample was added to their respective wells. The plate was then sealed, incubated, and shaken at room temperature for 1 hour, then washed three times. 25µL of Detection antibody Mix was added to each well, then the plate was sealed, incubated, and shaken at room temperature for 30 minutes. The plate was then washed again three times. 120µL of Reading Buffer was then added to each well, the plate was sealed again, incubated, and shaken at room temperature for 5 minutes. The plate was then read on the Cytation 5 imaging reader (BioTek, Winooski, VT). The following cytokines and chemokines were measured: granulocyte-macrophage colony-stimulating factor (GM-CSF), interferon gamma (IFNγ), interleukin 1 beta (IL-1β), IL-2, IL-4, IL-5, IL-6, IL-12p70, IL-13, IL-18, tumor necrosis factor alpha (TNFα), IL-9, IL-10, IL-17A, IL-22, IL-23, IL-27, eotaxin , growth related oncogene alpha (GROα), interferon gamma induced protein 10 (IP-10), monocyte chemoattractant protein

Table 2-5. Cell types and markers.

Cell Type	Markers
Microglia	$CD11b^{+}CD45^{int}$, then gated for activation with CX3CR1, F4/80, and CD206
Myeloid Cells	$CD11b^{+}CD45^{high}$, then gated for MHCII and CD80 for activation
Dendritic Cells	$CD11b^{+}CD45^{high}CD11c^{+}$
Monocytes	$CD11b^{+}CD45^{high}Ly6C^{high\ or\ low}$, then gated on CD115 for activation
Helper T Cells	$TCR\beta^{+}CD4^{+}$
Cytotoxic T Cells	$TCR\beta^{+}CD8^{+}$
B Cells	$CD19^{+}Ly6G^{-}$
Neutrophils	$CD19^{-}Ly6G^{+}$

1 (MCP-1), MCP-3, macrophage inflammatory protein 1-alpha (MIP-1α), MIP-β, MIP-2, and regulated on activation, normal T cell expressed and secreted (RANTES).

Serum Analysis

The serum sample concentrations were calculated using the Cytation 5 imaging reader and measured as pg/mL. The samples were plotted against the expected concentrations of the standard curve using the mean florescence intensity (MFI) of each standard. From this, the concentrations of the cytokines and chemokines were measured within the degree of sensitivity for each cytokine and chemokine. If the samples were measured below detection, they were recorded as 0 pg/mL. The measurements were then plotted, and significance between the BXD43 and B6 samples was calculated in GraphPad using a one-way ANOVA followed by Tukey's post comparison test. A value of $p < 0.05$ was considered significant and indicated by an asterisk.

CHAPTER 3. CAN THE BXD FAMILY BE USED TO DETERMINE EAE SUSCEPTIBILITY QTLS?

BXD Family of Mice

The BXD family of mouse strains is a useful tool for determining genetic variation in phenotypic traits. The BXD family is a series of recombinant inbred strains of mice from the parent strains B6 and D2. Isogenic F1 siblings are then interbred for several generations until distinct isogenic recombinant strains are produced, sharing different combinations of genetic sequences that can be traced back to the parent strains [55]. By testing these recombinant strains for disease traits, we may be able to identify QTLs that correlate with susceptibility, resistance, or other disease traits [56]. This makes the family invaluable in determining genetic factors that affect disease. GeneNetwork, a database of linked data sets that compare the genetic sequences of the BXD family of mice, can be used to analyze the results of these studies to determine potential QTLs for several traits.

It is necessary for us to test the parent strains for two reasons. First, it would be optimal for there to be a difference in how susceptible the two parent strains are to EAE for us to be able to identify genetic variation linked to EAE. If there is no difference in EAE susceptibility between the parent strains, then it is likely that EAE susceptibility would not be influenced by genetics. Second, we can test the degree of susceptibility or resistance of the parent strains in our animal facility to see if it matches the previous literature. Studies have shown that the B6 strain is susceptible to EAE through both passive and adoptive transfer using the MOG protein [47]. In contrast, the D2 strain has been shown to be resistant to developing EAE through the passive and adoptive transfer models [57].

For this study, we first tested the BXD parent strains, B6 and D2, for their susceptibility to EAE. We then recorded changes in body weight and disease score from day 7 to day 30 post-immunization. With these results, we then measured the following traits: incidence rate of EAE, average peak clinical score, average day of symptom onset, average length of acute onset (number of days the mice show symptoms), and average end score. We then looked at which BXD strains were able to develop EAE and to what degree of severity. We measured body weight change and clinical scores from day 7 to day 30 post-immunization. We measured the same traits in the BXD strains as previously mentioned for the parent strains. We then input these data into GeneNetwork to calculate potential QTLs for the following traits: incidence rate of EAE, average peak clinical score, average day of onset, average length of acute onset, and average end score. By entering that data into the database, genetic modifiers between strains can be identified.

BXD Parent Strains Vary in EAE Susceptibility

We tested the parent strains, B6 and D2, to determine if these strains would develop EAE. Historically, a dose of pertussis toxin has been used in the B6 strain of mice to increase the incidence rate of EAE, making the model more reliable for treatment studies. Additionally, pertussis toxin has also been used to induce EAE in mice that are historically resistant to developing EAE. However, it was decided to not utilize pertussis toxin in this EAE model to avoid identifying a QTL associated with PTX response. Thus, both B6 and D2 mice were immunized with an emulsion of CFA/MOG_{35-55} to induce EAE, then scored daily from day 7 to day 30. As shown in **Table 2-3**, our scoring criteria followed the Hooke Labs EAE scoring criteria. The mice were picked up each day and observed for paralysis symptoms: limp tail, inability to wrap tail around the researcher's finger, wobbly gait, dragging hind limbs, hind limb inhibition, and lack of movement. Additionally, the mice were weighed daily, and their weight changes were compared to the day of induction, as mice typically lose weight right before showing EAE symptoms. There were three criteria for humane euthanasia: 1) a mouse has lost 30% or more of its original body weight; 2) the mouse showed a score of 4 for 48 hours; and 3) the mouse showed a score of 4.5 or 5.

The results of this first study show a notable difference between the B6 mice and the D2 mice. The B6 mice were found to be susceptible to EAE after induction, with an average day of onset at day 15.6 (**Figure 3-1A**). The B6 mice showed an average peak score of 1.31 and maintained an average end score of 1.25 until day 30. These results are consistent with previous literature that shows the B6 strain exhibits a chronic model of EAE, where the mice get sick, reach a higher EAE score, then remain consistent the rest of the study [47]. In contrast, the D2 mice did not show any EAE symptoms, nor did they show any weight loss (**Figure 3-1B**). These results are also consistent with previous literature on the D2 strain [57]. With one parent strain susceptible to EAE and one strain not susceptible, we then tested the BXD offspring strains for susceptibility to EAE.

To investigate which BXD offspring strains were susceptible to EAE, we immunized a total of 16 BXD strains with a subcutaneous injection of CFA/MOG_{35-55} emulsion, with additional B6 mice as a positive control. Mice were then weighed and scored daily. After induction, 5 traits were calculated and the results were entered into GeneNetwork: incidence rate of EAE, average peak clinical score, average day of disease onset, average length of acute onset (or length of time the mouse is showing symptoms), and average end clinical score.

BXD Strains Vary in EAE Susceptibility and Severity

We tested 16 BXD strains by immunizing the mice with CFA/MOG. The following 6 strains developed EAE symptoms: BXD87, BXD48a, BXD43, BXD68, BXD125, and BXD75 (**Table 3-1**). The parent strain B6 showed an average peak clinical score of 0.68, with mice from the strains BXD43 and B6 reaching a disease severity of 4 (**Figure 3-2**). In comparison, the strains BXD87, BXD48, BXD68, and BXD125 only

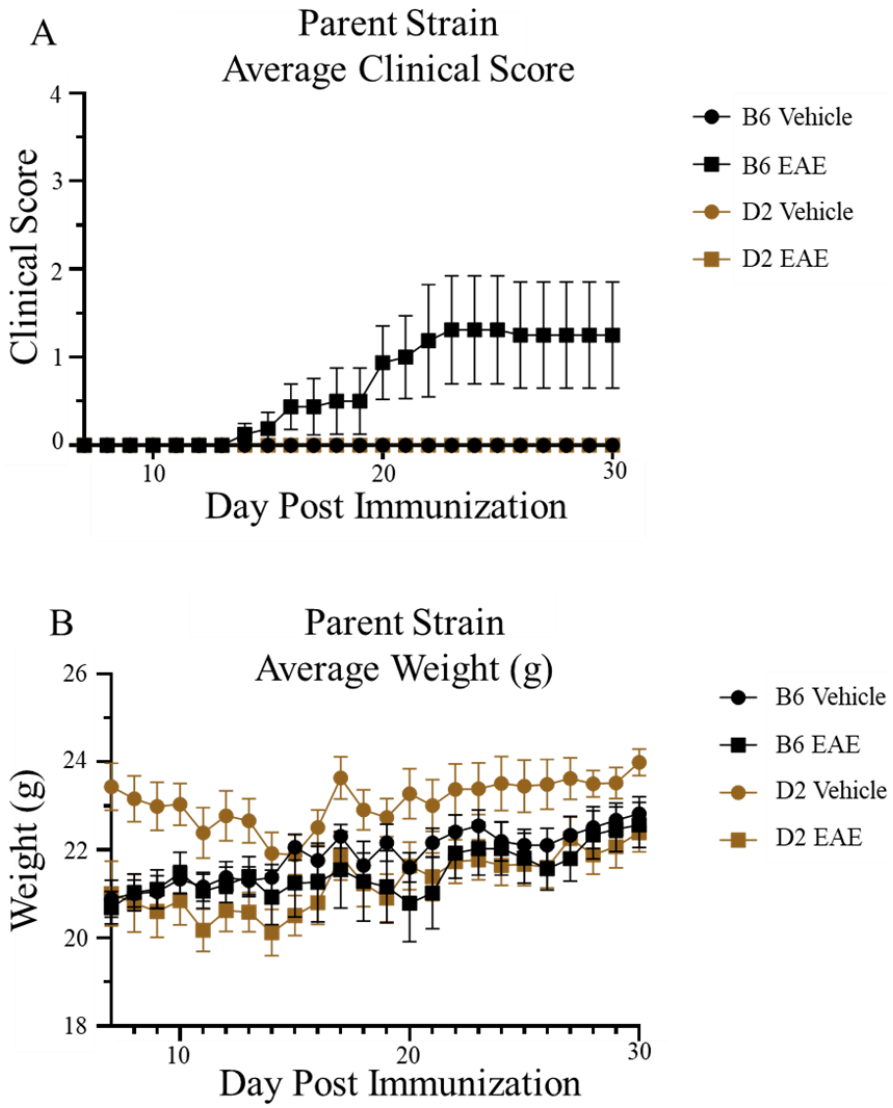

Figure 3-1. B6 mice develop EAE when induced with CFA/MOG$_{35-55}$, while D2 mice do not.

(A) Averaged EAE scores for each group. These results show that only the B6 mice that were induced with EAE showed disease symptoms; D2 mice induced with EAE did not develop disease. (B) Weight was recorded daily after day 7 post induction to monitor any weight loss related to developing EAE. A slight weight decrease for the B6 group with EAE is seen at the same time the mice start showing symptoms.

Table 3-1. BXD strain induction results.

Strain	N	Incidence Rate (%)	Average Peak Clinical Score	Average Day of Onset (EAE mice only)	Average End Score	Total Disease Severity Score (IR+ APCS+ AES)
C57BL/6 (B6)	14	0.57	0.821 ± 1.33	18.8 ± 3.25	0.71 ± 1.3	1.96
DBA/2J (D2)	8	0.00	0 ± 0	0 ± 0	0 ± 0	0
BXD77	4	0.00	0 ± 0	0 ± 0	0 ± 0	0
BXD79	3	0.00	0 ± 0	0 ± 0	0 ± 0	0
BXD44	4	0.00	0 ± 0	0 ± 0	0 ± 0	0
BXD87	4	0.75	0.38 ± 0.25	20 ± 0.58	0.13 ± 0.13	1.25
BXD48a	4	0.75	0.38 ± 0.25	17 ± 0	0.13 ± 0.13	1.25
BXD73b	4	0.00	0 ± 0	0 ± 0	0 ± 0	0
BXD89	4	0.00	0 ± 0	0 ± 0	0 ± 0	0
BXD43	7	0.86	3.64 ± 2.32	14.83 ± 0.75	3.57 ± 2.44	8.07
BXD68	4	0.50	0.25 ± 0.29	17 ± 0	0 ± 0	0.75
BXD125	4	0.50	0.25 ± 0.29	17 ± 0	0 ± 0	0.75
BXD90	4	0.00	0 ± 0	0 ± 0	0 ± 0	0
BXD11	4	0.00	0 ± 0	0 ± 0	0 ± 0	0
BXD213	4	0.00	0 ± 0	0 ± 0	0 ± 0	0
BXD170	4	0.00	0 ± 0	0 ± 0	0 ± 0	0
BXD75	4	0.50	0.5 ± 1.33	16 ± 0	0.25 ± 0.25	1.25
BXD55	4	0.00	0 ± 0	0 ± 0	0 ± 0	0
All groups			P= 0.0004	P= 0.366	P= 0.0003	

Mean ± Standard Deviation. N: number of mice. IR: Incidence Rate. APCS: Average Clinical Peak Score. AES: Average End Score. One-way Analysis of Variance (ANOVA) followed by Tukey's post comparison test to compare mean of each group to all other groups.

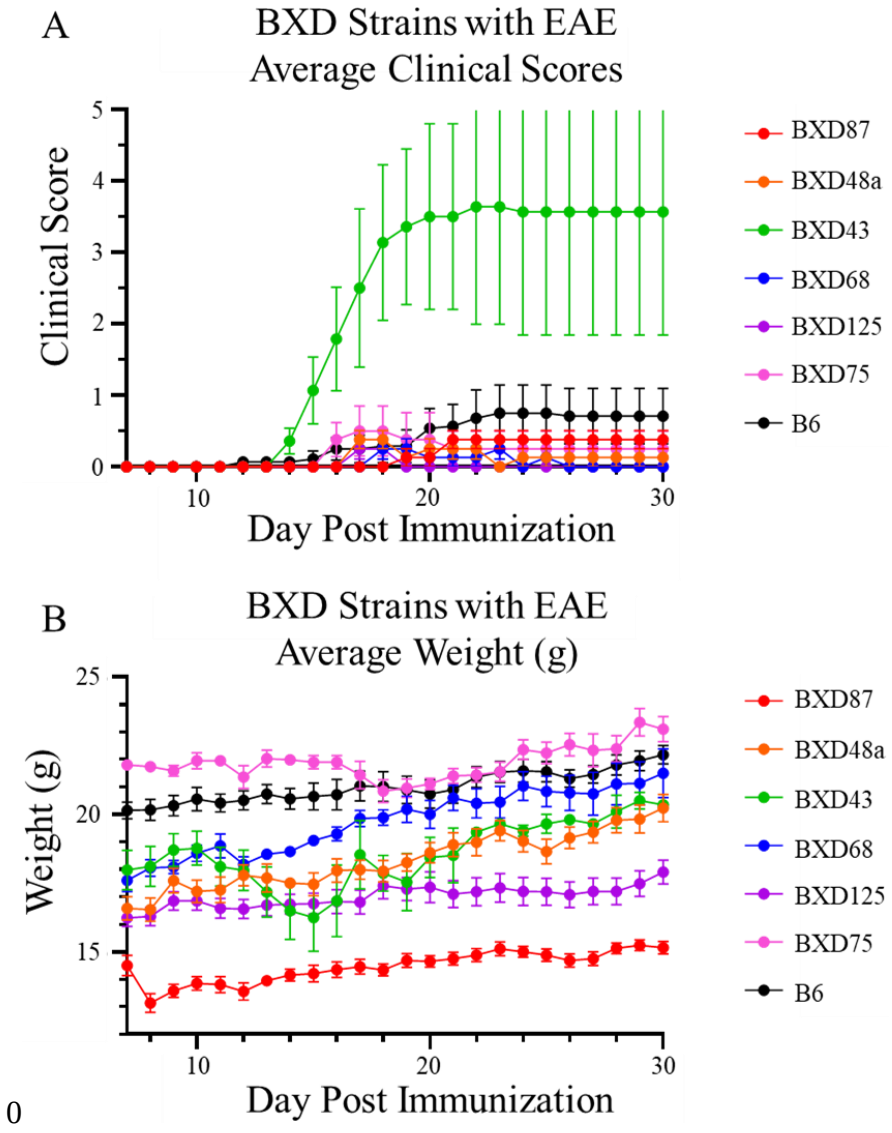

Figure 3-2. BXD strains that develop EAE show varying severity.

(A) Scores were measured daily between day 7 and day 30. The strain BXD43 began to show EAE symptoms at an earlier day and showed a rapid increase in disease severity. (B) Weight was measured daily from day 7 post induction to day 30. The only strain that shows a notable dip in weight before symptoms begin is BXD43.

developed a disease severity score of 0.5. The average peak clinical scores of these strains range from 0.38-0.25. The BXD75 strain showed a slightly higher disease burden, with an average peak clinical score of 0.5, and reaching a maximum disease score of 1.5. Finally, the strain BXD43 showed an average peak clinical score of 2.93, with a maximum clinical score of 4.5. The changes in weight for the susceptible strains, as well as the clinical scores, were found to be significantly different (**Tables 3-2** and **3-3**), showing that there is a noteworthy difference between the BXD strains.

Using the clinical scoring data, we calculated the average final clinical score for each BXD strain. The parent strain B6 showed an average final score of 0.64, while the strains BXD87 and BXD48a showed an average final score of 0.13 (**Figure 3-2A**). The strain BXD75 showed an average final score of 0.25, while the strains BXD68 and BXD125 showed an average final score of 0. Finally, the strain BXD43 showed an average final score of 3.6. Based on these results, it is a bit difficult to categorize most of the strains as either chronic or relapsing remitting EAE, as the mice do not show a pattern of relapse and remission. For the strains BXD87 and BXD48a, only one mouse went from a score of 0.5 to 0, while the other sick mice stayed at a score of 0.5. However, despite these relatively now EAE scores, all 6 strains showed an incidence rate of at least 50%, with BXD87 and BXD48a showing an incidence rate of 75%. BXD43 showed an incidence rate of 86% (**Figure 3-3A**).

The BXD strains also showed variability in disease progression. The sick mice in BXD68 and BXD125 returned to a score of zero. In contrast, the strain BXD75 had one mouse reach a score of 0.5, then return to 0, while another reached a score of 1.5, then regressed to a score of 1 for the rest of the study. This suggests that the strain BXD75 may exhibit a chronic model of EAE. In chronic EAE a mouse gets sick, increases in disease severity, then regresses a bit in score and stays consistent until the end of a study and does not exhibit any relapse-remitting pattern. Additionally, the strain BXD43 showed a rapidly increasing disease severity, with most sick mice ranging from a score of 0.5 to 4.5 in an average 4.2 days. As the mice had to be euthanized, it could not be determined if the mice would regress in severity. Future studies may investigate reducing disease severity in the BXD43 strain to determine if the mice exhibit a chronic or relapsing-remitting model. However, the rapid severity of EAE in BXD43 may serve as a useful model for rapidly progressing EAE, and thus, may serve as a model for PPMS.

The average day of onset after induction was also measured with the susceptible strain. The parent strain B6 showed an average day of onset of day 18.8. The strain BXD75 showed an average day of onset of day 16, while BXD48a, BXD68, and BXD125 all showed an average day of onset of day 17. The strain BXD87 showed an average day of onset of day 20, while BXD43 showed an average day of onset of day 14.8 (**Table 3-1**). Based on these results, BXD43 mice are shown to begin exhibiting symptoms much more quickly than other strains, while most strains show a similar day of onset to that of the parent strain B6.

Table 3-2. Average weight for BXD strains susceptible to EAE.

Day after Induction	BXD87	BXD48a	BXD43	BXD68	BXD125	BXD75	B6
7	14.50 ± 0.74	16.58 ± 0.85	17.97 ± 1.91	17.60 ± 0.80	16.23 ± 0.64	21.80 ± 0.27	20.14 ± 1.08
8	13.13 ± 0.67	16.53 ± 0.85	18.10 ± 1.93	18.05 ± 0.60	16.28 ± 0.68	21.73 ± 0.26	20.16 ± 1.40
9	13.58 ± 0.48	17.58 ± 0.90	18.70 ± 1.57	18.08 ± 0.48	16.85 ± 0.68	21.58 ± 0.39	20.31 ± 1.36
10	13.85 ± 0.51	17.20 ± 0.84	18.76 ± 1.64	18.58 ± 0.60	16.85 ± 0.68	21.95 ± 0.59	20.55 ± 1.53
11	13.80 ± 0.59	17.25 ± 0.94	18.09 ± 1.88	18.85 ± 0.87	16.58 ± 0.71	21.95 ± 0.19	20.41 ± 1.19
12	13.55 ± 0.64	17.78 ± 0.76	17.96 ± 2.00	18.18 ± 0.54	16.55 ± 0.70	21.35 ± 0.83	20.51 ± 1.24
13	13.95 ± 0.31	17.68 ± 1.02	17.17 ± 2.42	18.55 ± 0.06	16.70 ± 0.78	22.03 ± 0.61	20.74 ± 1.27
14	14.15 ± 0.44	17.50 ± 0.36	16.49 ± 2.76	18.65 ± 0.35	16.73 ± 0.73	21.98 ± 0.17	20.56 ± 1.38
15	14.20 ± 0.61	17.45 ± 0.83	16.24 ± 3.23	19.05 ± 0.13	16.75 ± 0.75	21.90 ± 0.48	20.65 ± 1.77
16	14.35 ± 0.58	17.95 ± 0.86	16.85 ± 3.19	19.28 ± 0.50	16.83 ± 0.88	21.90 ± 0.48	20.71 ± 1.99
17	14.45 ± 0.55	17.98 ± 0.69	18.53 ± 2.49	19.85 ± 0.58	16.80 ± 0.88	21.43 ± 1.00	21.03 ± 1.95
18	14.33 ± 0.45	17.93 ± 0.79	17.85 ± 1.30	19.88 ± 0.57	17.40 ± 0.96	20.85 ± 0.84	21.01 ± 1.95
19	14.68 ± 0.49	18.25 ± 0.64	17.53 ± 2.09	20.18 ± 0.95	17.28 ± 0.85	20.95 ± 0.68	20.89 ± 1.79
20	14.65 ± 0.42	18.60 ± 0.74	18.43 ± 1.25	20.00 ± 1.01	17.35 ± 1.14	21.10 ± 0.42	20.74 ± 1.86
21	14.75 ± 0.47	18.90 ± 0.88	18.50 ± 1.73	20.60 ± 0.91	17.10 ± 0.99	21.40 ± 0.55	20.90 ± 1.78
22	14.88 ± 0.49	18.98 ± 0.97	19.35 ± 0.21	20.40 ± 1.06	17.18 ± 1.02	21.43 ± 0.51	21.36 ± 1.33
23	15.10 ± 0.50	19.40 ± 0.74	19.65 ± 0.07	20.45 ± 1.16	17.33 ± 1.04	21.55 ± 0.70	21.54 ± 1.34
24	15.00 ± 0.41	19.03 ± 0.79	19.40 ± 0.28	21.03 ± 1.03	17.20 ± 1.02	22.35 ± 0.71	21.58 ± 1.42
25	14.88 ± 0.46	18.65 ± 0.89	19.65 ± 0.49	20.83 ± 1.11	17.18 ± 0.99	22.23 ± 0.78	21.55 ± 1.28
26	14.68 ± 0.49	19.15 ± 0.79	19.80 ± 0.14	20.78 ± 1.27	17.08 ± 0.95	22.53 ± 0.83	21.30 ± 1.11
27	14.75 ± 0.51	19.35 ± 0.77	19.65 ± 0.21	20.75 ± 1.56	17.20 ± 0.99	22.33 ± 1.18	21.45 ± 1.11
28	15.13 ± 0.40	19.78 ± 0.93	20.10 ± 0.85	21.10 ± 1.52	17.20 ± 0.99	22.38 ± 0.95	21.80 ± 1.29
29	15.23 ± 0.39	19.83 ± 1.01	20.50 ± 0.42	21.13 ± 1.57	17.48 ± 0.93	23.35 ± 1.01	21.95 ± 1.25
30	15.15 ± 0.45	20.23 ± 0.99	20.35 ± 0.21	21.50 ± 1.78	17.90 ± 0.88	23.10 ± 0.92	22.17 ± 1.19
All groups	**P= <0.001**						
Against BXD43	**P= <0.001**	P= 0.803	N/A	**P= <0.001**	**P= <0.001**	**P= <0.001**	**P= <0.001**

Mean ± Standard Deviation. One-way ANOVA followed by Tukey's post comparison test to compare mean of each group to the strain BXD43.

Table 3-3. Average clinical score of BXD strains susceptible to EAE

Day after Induction	BXD87	BXD48a	BXD43	BXD68	BXD125	BXD75	B6
7	0 ± 0	0 ± 0	0 ± 0	0 ± 0	0 ± 0	0 ± 0	0 ± 0
8	0 ± 0	0 ± 0	0 ± 0	0 ± 0	0 ± 0	0 ± 0	0 ± 0
9	0 ± 0	0 ± 0	0 ± 0	0 ± 0	0 ± 0	0 ± 0	0 ± 0
10	0 ± 0	0 ± 0	0 ± 0	0 ± 0	0 ± 0	0 ± 0	0 ± 0
11	0 ± 0	0 ± 0	0 ± 0	0 ± 0	0 ± 0	0 ± 0	0 ± 0
12	0 ± 0	0 ± 0	0 ± 0	0 ± 0	0 ± 0	0 ± 0	0.071 ± 0.18
13	0 ± 0	0 ± 0	0 ± 0	0 ± 0	0 ± 0	0 ± 0	0.071 ± 0.18
14	0 ± 0	0 ± 0	0.36 ± 0.48	0 ± 0	0 ± 0	0 ± 0	0.071 ± 0.27
15	0 ± 0	0 ± 0	1.07 ± 1.24	0 ± 0	0 ± 0	0 ± 0	0.11 ± 0.40
16	0 ± 0	0 ± 0	1.79 ± 1.78	0 ± 0	0 ± 0	0.38 ± 0.48	0.25 ± 0.58
17	0 ± 0	0.38 ± 0.25	2.50 ± 2.22	0 ± 0	0.25 ± 0.29	0.50 ± 0.71	0.25 ± 0.70
18	0 ± 0	0.38 ± 0.25	3.14 ± 2.17	0.25 ± 0.29	0.25 ± 0.29	0.50 ± 0.71	0.29 ± 0.83
19	0.13 ± 0.25	0.13 ± 0.25	3.36 ± 2.17	0.25 ± 0.29	0 ± 0	0.38 ± 0.75	0.29 ± 0.83
20	0.13 ± 0.25	0.25 ± 0.29	3.50 ± 2.25	0.13 ± 0.25	0 ± 0	0.38 ± 0.75	0.54 ± 0.99
21	0.38 ± 0.25	0.25 ± 0.29	3.50 ± 2.25	0.13 ± 0.25	0 ± 0	0.25 ± 0.50	0.57 ± 1.11
22	0.38 ± 0.25	0.25 ± 0.29	3.64 ± 2.32	0.13 ± 0.25	0 ± 0	0.25 ± 0.50	0.68 ± 1.38
23	0.38 ± 0.25	0 ± 0	3.64 ± 2.32	0.25 ± 0.29	0 ± 0	0.25 ± 0.50	0.75 ± 1.37
24	0.38 ± 0.25	0.13 ± 0.25	3.57 ± 2.44	0 ± 0	0 ± 0	0.25 ± 0.50	0.75 ± 1.37
25	0.38 ± 0.25	0.13 ± 0.25	3.57 ± 2.44	0.13 ± 0.25	0 ± 0	0.25 ± 0.50	0.75 ± 1.37
26	0.38 ± 0.25	0.13 ± 0.25	3.57 ± 2.44	0 ± 0	0 ± 0	0.25 ± 0.50	0.71 ± 1.34
27	0.38 ± 0.25	0.13 ± 0.25	3.57 ± 2.44	0 ± 0	0 ± 0	0.25 ± 0.50	0.71 ± 1.34
28	0.38 ± 0.25	0.13 ± 0.25	3.57 ± 2.44	0 ± 0	0 ± 0	0.25 ± 0.50	0.71 ± 1.34
29	0.38 ± 0.25	0.13 ± 0.25	3.57 ± 2.44	0 ± 0	0 ± 0	0.25 ± 0.50	0.71 ± 1.34
30	0.38 ± 0.25	0.13 ± 0.25	3.57 ± 2.44	0 ± 0	0 ± 0	0.25 ± 0.50	0.71 ± 1.34
All groups	**P= <0.001**						
Against BXD43	**P= <0.001**	**P= <0.001**	N/A	**P= <0.001**	**P= <0.001**	**P= <0.001**	**P= <0.001**

Mean ± Standard Deviation. One-way ANOVA followed by Tukey's post comparison test to compare mean of each group to the strain BXD43. A bolded P value is considered significant ($P<0.05$)

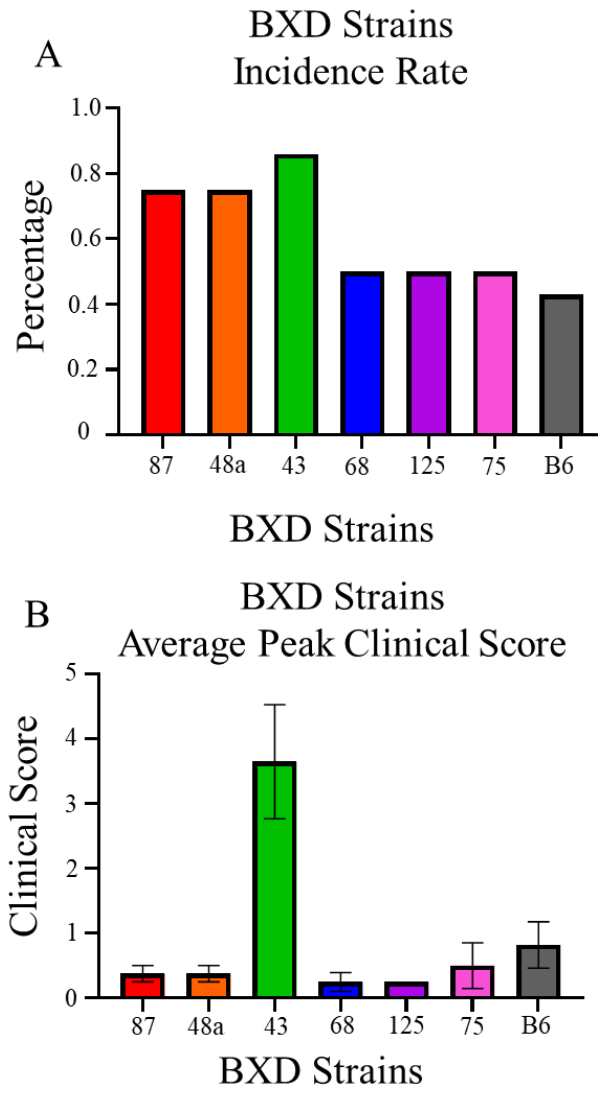

Figure 3-3. 6 BXD strains were found susceptible to EAE.

(A) Incidence rate of EAE in each BXD strain. (B) Average peak clinical score of each BXD strain that develops EAE. The highest EAE score of each mouse was recorded then averaged.

These results show that while several BXD mouse strains can develop EAE following CFA/MOG_{35-55} immunization, most mice only showed a very mild disease burden. This is reflected in the parent strain B6, which historically has shown varying disease severity. Due to the study only lasting 30 days, we cannot determine any patterns in disease presentation that would suggest a chronic model or a relapsing-remitting model. One study for future research would be to continue past 30 days to see if there is any evidence of relapsing in some of the mice. Notably, the strain BXD43 showed an extremely heavy disease burden, with the majority of the sick mice developing a clinical of 4.5 before reaching the humane endpoint. The strain also showed the highest incidence rate. This suggests that the BXD43 strain may serve as an effective extreme phenotype model.

GeneNetwork Quantitative Trait Loci Mapping

The trait data collected from the BXD strains immunized with CFA/MOG was entered into the gene database GeneNetwork to determine if any QTLs could be identified. The database contains the entire gene sequences of every BXD strain, and thus by entering data for individual strains, the database can calculate the likelihood ratio statistic (LRS) that there is a QTL at that specific allele.

A total of 5 traits were measured and the results were entered into GeneNetwork and analyzed via interval mapping (**Figure 3-4**). The first trait measured was the final clinical score. The results from GeneNetwork, as shown in Figure 5-3, show several suggestive QTLs, with the highest likelihood ratio statistic (LRS) being for alleles on chromosomes 5 and 17 (**Figure 3-4A**). The next trait was the average day of onset of EAE, and there were no results that surpassed the threshold for a suggestive QTL (**Figure 3-4B**). The third trait tested was incidence rate in female mice, and the results found a suggestive QTL on chromosome 5 (**Figure 3-4C**). The fourth trait tested was length of acute disease, and the results found two suggestive QTLs on chromosome 5 and chromosome 11 (**Figure 3-4D**). Finally, the last trait tested was peak clinical score, and the results found one suggestive QTLs on chromosome 5 (**Figure 3-4E**). Taken together, these results suggest that certain genes found on chromosomes 5, 11, and 18 may determine these measured traits. However, due to the small sample and BXD strain number, none of the results showed a significant QTL. Future studies will be needed to increase the number of tested strains and further refine the QTLs predicted.

The wide range in disease susceptibility between the different BXD strains shows how much even genetic differences may influence EAE susceptibility and severity. With the addition of more BXD strains tested in the future, it may be possible to further narrow down possible QTLs for EAE susceptibility, EAE severity, and length of onset. Future studies may investigate increasing the length of observation on the mice that are showing EAE symptoms, as longer studies may help identify if certain strains exhibit chronic or relapsing remitting EAE. These studies lay the groundwork for identifying genetic factors that determine EAE susceptibility in the BXD family of mice, which may help identify possible candidates for equivalent genes for MS.

Figure 3-4. BXD mice may express QTLs for developing EAE on chromosomes 5 and 11.

Whole genome mapping from GeneNetwork for the following traits: (A) clinical score at day 30, (B) day of onset for EAE, (C) incidence rate in female mice, (D) length of acute disease, (E) and peak clinical score. The maps were calculated using interval mapping with 1000 tests.

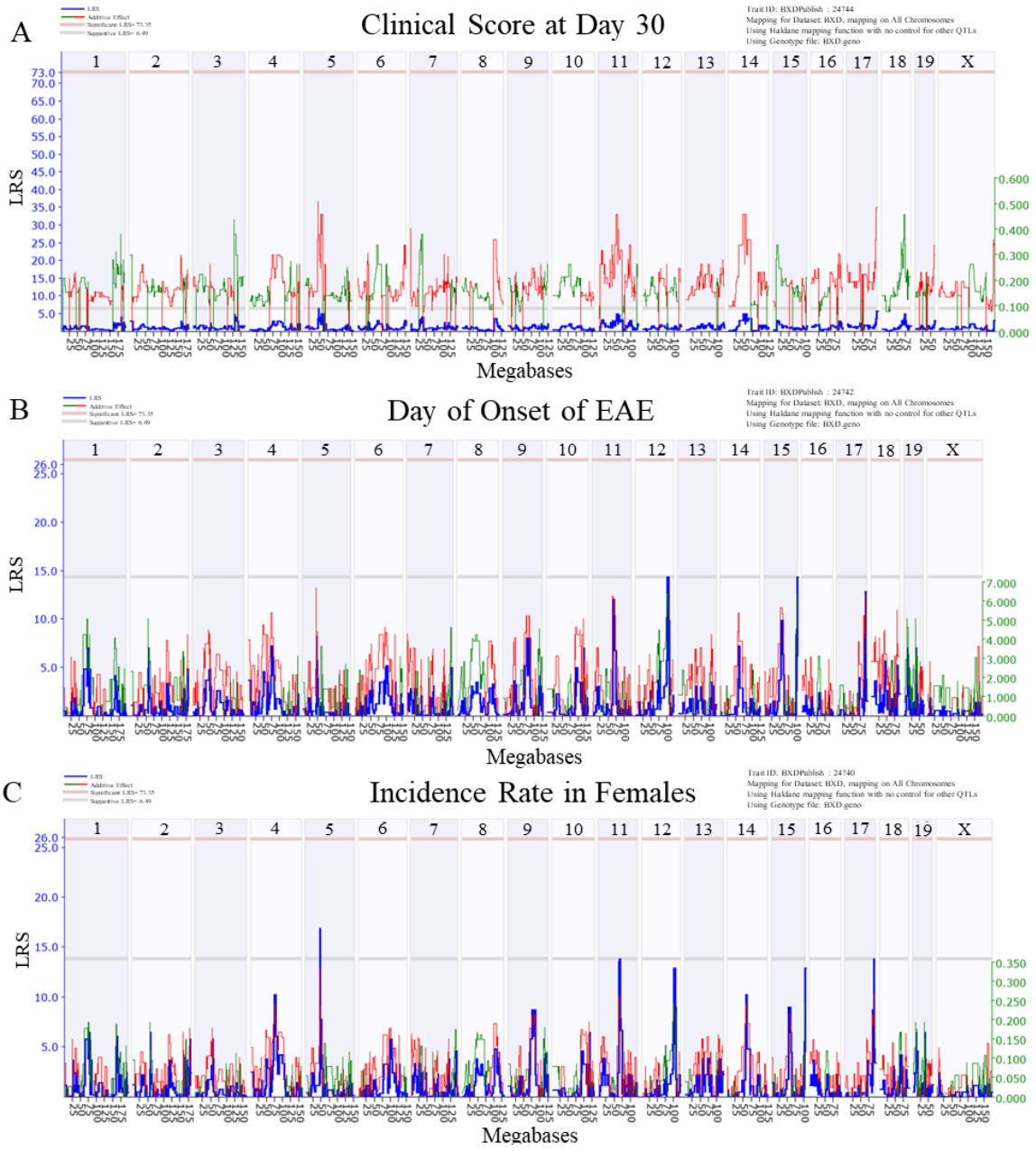
A
Clinical Score at Day 30
Trait ID: BXDPublish : 24744
Mapping for Dataset: BXD, mapping on All Chromosomes
Using Haldane mapping function with no control for other QTLs
Using Genotype file: BXD.geno
LRS
Megabases
B
Day of Onset of EAE
Trait ID: BXDPublish : 24742
Mapping for Dataset: BXD, mapping on All Chromosomes
Using Haldane mapping function with no control for other QTLs
Using Genotype file: BXD.geno
LRS
Megabases
C
Incidence Rate in Females
Trait ID: BXDPublish : 24740
Mapping for Dataset: BXD, mapping on All Chromosomes
Using Haldane mapping function with no control for other QTLs
Using Genotype file: BXD.geno
LRS
Megabases

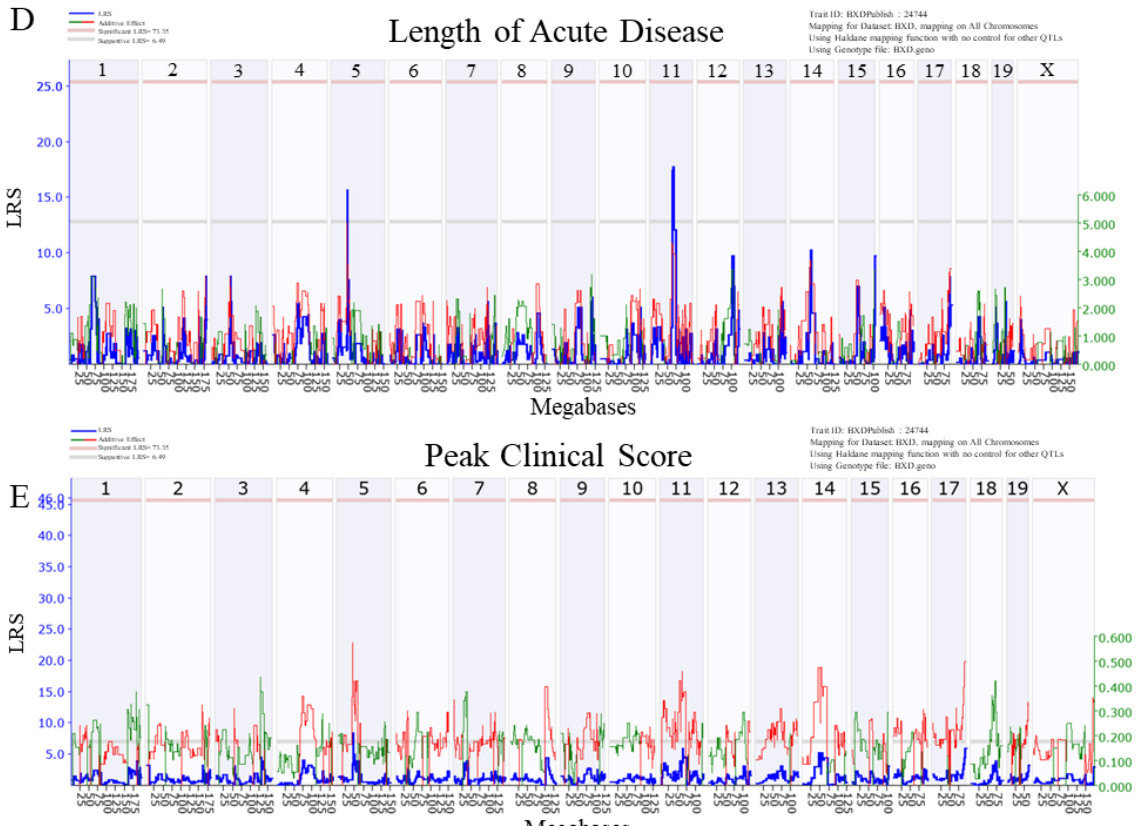

Figure 3-4. (Continued).

CHAPTER 4. WHAT ARE THE CHARACTERSISTICS OF THE BXD43 STRAIN AS AN EXTREME PHENOTYPE?

The results of the induction studies showed that the strain BXD43 showed an extreme phenotype of EAE disease severity. The next goal was to determine what was unique about the BXD43 strain that resulted in such a severe form of EAE. We established a breeding colony for the BXD43 strain of mice to characterize the development of EAE in comparison to the B6 strain. For this study, we first induced both BXD43 and B6 mice, then measured their disease progression from day 7 to day 15 for the BXD43 mice and day 19 for the B6 mice in the first study, then day 29 for the B6 mice in the second study. Day 15 was found to be the average day of EAE development for the BXD strain of mice, and waiting longer would risk the mice having to be euthanized prematurely. We waited until day 29 for the B6 mice with EAE to see if the mice would eventually develop symptoms, but the mice in this group never showed symptoms. We then measured the immune cell populations in the spinal cords of each group of mice to compare changes to the CNS. Finally, we measured changes in the cytokine and chemokine levels in serum samples from both BXD43 and B6 mice.

Changes in Spinal Cord Cell Populations in BXD43 Mice

A characteristic feature of EAE pathology is infiltration of the CNS by inflammatory immune cells, which then begin to attack myelin proteins, resulting in paralysis. Over time, the spinal cord develops lesions that contain high numbers of inflammatory monocytes, lymphocytes, and macrophages, similarly to how lesions develop in the brains of MS patients. Therefore, comparison of immune cell infiltrates from spinal cords of mice with EAE has been an indication of disease severity. For the first study, we immunized the mice with an emulsion of via CFA/MOG_{35-55} and compared BXD43 mice with B6 mice. We then observed the mice from day 7 to the day 15 for the BXD43 mice and day 19 for the B6 mice, which were the average day of peak disease severity for the BXD43 mice and the B6 mice, respectively. The spinal cords were then harvested, homogenized, and stained for microglia, myeloid cells, and lymphocytes.

However, in this first study, the B6 mice never showed EAE symptoms, which made it difficult to compare cell populations between the two strains (**Figure 4-1A**). Three of the four BXD43 mice induced with EAE developed a score of 3 or higher by day 15 and showed weight loss as symptoms progressed. None of the B6 EAE mice showed any symptoms, nor did they show any weight loss. This study demonstrated the need for a B6 group of mice that would more reliably develop EAE symptoms. Thus, for the rest of the studies, we included a group of B6 mice that were immunized with CFA/MOG_{35-55} and received a PTX dose 2 hours after induction, as well as on day 1. This increased the incidence rate of the B6 mice, allowing us to better compare the B6 and BXD43 mice.

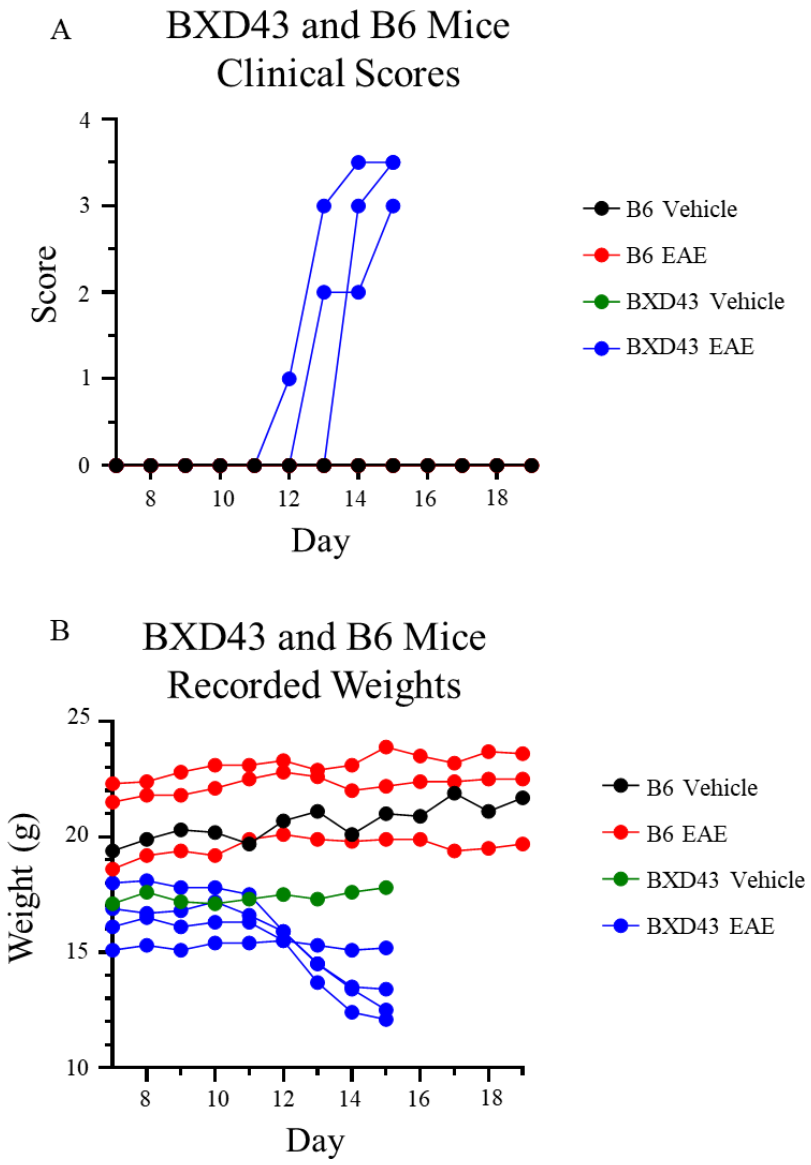

Figure 4-1. BXD43 mice show a higher susceptibility to EAE than B6 mice.

(A) EAE clinical scores of BXD43 and B6 mice from day 7 post induction to day 19. Only 3 of 4 BXD43 mice induced with EAE developed symptoms, and none of the B6 mice induced with EAE developed symptoms. (B) Weights of BXD43 and B6 mice from day 7 post induction to day 19. All the BXD43 mice showed weight loss as symptoms developed, but none of the B6 mice showed any weight loss.

This led us to repeat the study a second time with a fifth group of B6 mice with EAE and were dosed with PTX to create a better positive control to compare the BXD43 mice to. Therefore, the second study had five groups: BXD43 with PBS/vehicle, BXD43 with EAE, B6 with PBS/vehicle, B6 with EAE, and B6 with EAE+PTX. In this second study, the BXD43 mice, as well as the B6 mice with EAE+PTX and one B6 with PBS/mock, were euthanized and spinal cords were collected on day 15. The rest of the B6 mice were harvested on day 29, as we waited to see if the B6 mice with EAE alone would develop symptoms. Spinal cord cells were then measured and gated for microglial cells, myeloid cells, and lymphoid cells using flow cytometry, and the results were measured using FlowJo to calculate cell population percentages.

In the second study, two out of three mice from the BXD43 mice with EAE developed symptoms, reaching maximum scores of 1.5 and 2.5 on day 14 (weights and scores were not recorded on day of harvest) (**Figure 4-2A**). Additionally, two out of three mice from the B6 mice with EAE+PTX also developed symptoms, reaching maximum scores of 3.5 and 2. The B6 mice with EAE only were then left until day 29 to see if they would develop any symptoms, along with one B6 mouse with PBS/vehicle to serve as a control. However, none of the B6 mice with EAE alone developed any symptoms by day 29.

Based on the results of these studies, the BXD43 strain shows a similar incidence rate and disease severity to the B6 mice when induced with CFA/MOG and dosed with PTX. This suggests the BXD43 strain may serve as a reliable model for EAE that is not influenced by external factors such as PTX dosing. After this, we measured changes in the spinal cord and cytokine/chemokine levels in the peripheral blood.

Increased Immune Cell Infiltration in BXD43 Mice

To identify the immune cell populations in the spinal cord of the BXD43 and B6 mice immunized with MOG, we used flow cytometry. The spinal cord cells were stained with antibodies to immune cell markers and analyzed on a flow cytometer. The cells were gated to exclude doublets and then gated with CD11b on the x axis and CD45 on the y axis, creating three immune cell populations (**Figure 4-3A**). The first group, $CD11b^{-}$ $CD45^{+}$ cells, contained lymphocyte populations and labeled as group R1 (**Figure 4-3B**). The second group, $CD11b^{+}CD45^{high}$ cells, were identified as myeloid cells and labeled as group R2. The last group, $CD11b^{+}CD45^{mid}$ cells, contained microglia and were labeled as R3. This gating was used for identifying myeloid cells and microglia cells. For the third group, a second gating strategy was used to identify lymphocyte populations to distinguish T cells and B cells. The spinal cord cells were stained for TCRβ and CD19, respectively. $TCR\beta^{+}$ cells were identified as T cells, while $CD19^{+}$ cells were identified as B cells.

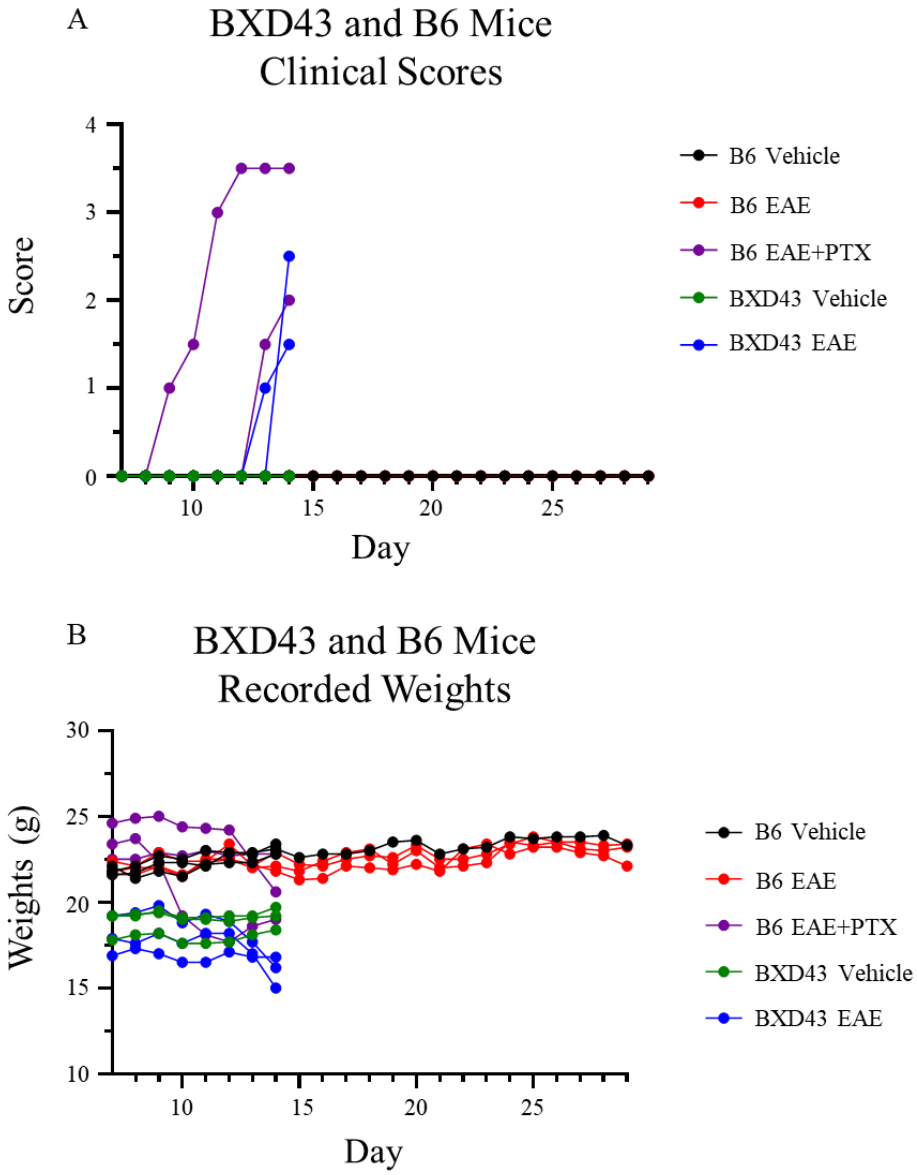

Figure 4-2. BXD43 mice show a similar incidence rate of EAE to B6 mice when dosed with pertussis toxin.

(A) EAE clinical scores in BXD43 and B6 mice from day 7 post induction to day 29. Both BXD43 mice with EAE and B6 mice with EAE+PTX developed symptoms. (B) Weights of BXD43 and B6 mice from day 7 post induction to day 29. The mice that showed symptoms also showed weight loss as symptoms developed.

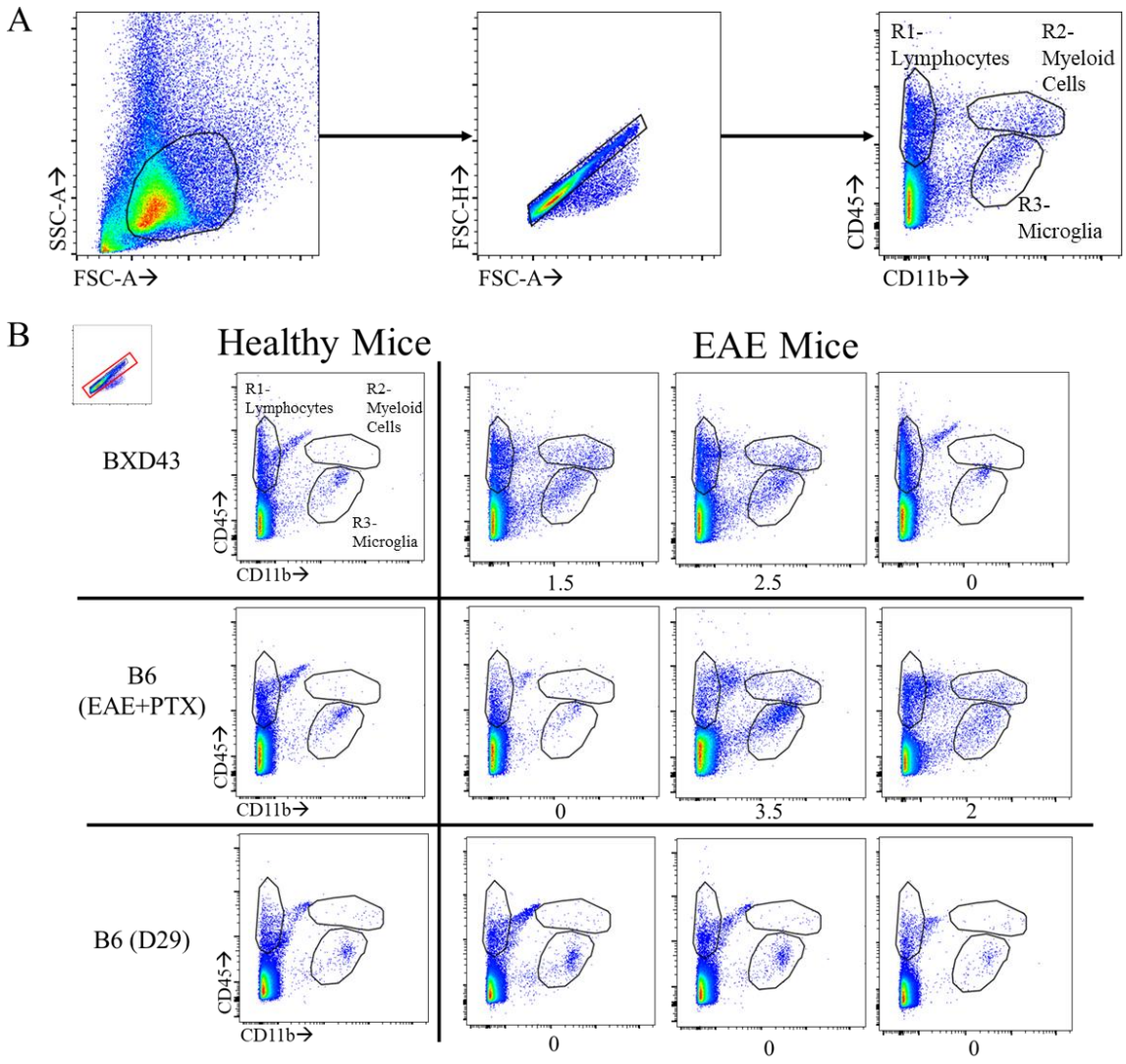

Figure 4-3. Both BXD43 and B6 mice with EAE have a higher population of myeloid cells and microglia in the spinal cord than healthy mice.

(A) Gating strategy for identifying myeloid cells and microglia in the spinal cord of BXD43 and B6 mice with EAE. Myeloid cells and microglia were identified using the cell markers CD11b and CD45. (B) Comparison of myeloid and microglial cells in BXD43 mice and B6 mice. The three graphs on the left show the control mice, while the nine graphs on the right show the induced mice and their respective EAE scores. In both BXD43 and B6 mice, a higher EAE score correlates with a higher population of myeloid cells and microglia.

We compared the number of cells in each immune cell population to determine differences between the BXD43 and B6 mice with EAE. In both the BXD43 and B6 strains, mice with EAE showed a trend towards a higher population of overall immune cells in the spinal cord than healthy mice, showing that EAE does induce immune cell infiltration into the spinal cord (**Figure 4-3B**). Additionally, the immune cell population in the BXD43 was more similar to the B6 mice with EAE and pertussis toxin dosing than that of the B6 with EAE alone (**Table 4-1**). The BXD43 mice that were induced with EAE showed a slightly higher level of expression of F4/80, though not enough to be considered significant. Interestingly, while B6 mice with EAE+PTX showed a trend of higher levels of CX_3CR1 than healthy B6 mice, healthy BXD43 mice showed a trend of a higher expression of CX_3CR1 (**Table 4-2**). This suggests that even healthy BXD43 microglia may already express a phenotype found in EAE in other mice strains, which might contribute to the rapid and severe progression of EAE in the BXD43 mice.

Changes in Microglia Cells in BXD43 Mice

We measured the expression of microglial cell markers from the R3 gate in the BXD43 and B6 mice. The microglial cells were gated to show CX_3CR1 vs F4/80 cells (**Figure 4-4B**). Next, microglial cells were gated to show CX_3CR1 vs CD206 cells (**Figure 4-4C**).

The microglial cells in the BXD43 and B6 mice with EAE were then analyzed to determine differences in cell counts between the groups. There was a significant difference between the BXD43 EAE mice and the BXD43 Control mice in expression of $CX_3CR1^+F4/80^-$ cells, with the BXD43 EAE mice showing a lower percentage of $CX_3CR1^+F4/80^-$ cells (Table 4-2). There was a trend towards the BXD43 EAE mice showing a lower expression of CX_3CR1+ microglia. There was no significant difference between the microglia populations of the BXD43 EAE mice and the B6 EAE+PTX mice.

Changes in Myeloid Cell Populations of BXD43 Mice

We gated out myeloid cells for both the BXD43 and B6 mice with EAE. The myeloid cells were gated for MHCII and CD80 to show activated cells. Next, the myeloid cells were gated for Ly6C vs MHCII to show activated monocytes (**Figure 4-5B**). The myeloid cells were also gated for Ly6C vs CD80 to show activated monocytes (**Figure 4-5C**).

We compared the cell counts for the different myeloid cell populations for the spinal cord samples from the BXD43 and B6 mice with EAE. Induction of EAE was shown to increase the percentage of inflammatory and active monocytes in both BXD43 and B6 mice (**Figure 4-5B**), identified as $Ly6C^+$ and $CD80^+$ cells. The BXD43 EAE mice showed a slightly higher population of $Ly6C^+$ cells than the BXD43 Control mice, though not enough to be considered significant. The BXD43 mice with EAE showed a trend of a greater percentage of $Ly6C^+$ cells compared to the B6 EAE+PTX mice but was not

Table 4-1. Both BXD43 mice with EAE and B6 mice with EAE+PTX show higher percentages of myeloid cells and microglia.

Groups	Myeloid Cells (R2)	Microglia (R3)
BXD43 (Mock)	0.10 ± 0.09	0.55 ± 0.33
BXD43 EAE	0.67 ± 0.47	1.06 ± 0.48
B6 (Mock)	0.04 ± 0.01	0.47 ± 0.10
B6 EAE	0.06 ± 0.02	0.46 ± 0.21
B6 EAE+PTX	0.56 ± 0.39	1.50 ± 1.32
One-way ANOVA comparing all groups	**P= 0.045**	P= 0.282
BXD43 (Mock) and B6 (Mock)	P= >0.999	P= >0.999
BXD43 (Mock) and B6 EAE	P= >0.999	P= >0.999
BXD43 (Mock) and B6 EAE+PTX	P= 0.518	P= 0.439
BXD43 EAE and B6 (Mock)	P= 0.175	P= 0.799
BXD43 EAE and B6 EAE	P= 0.195	P= 0.789
BXD43 EAE and B6 EAE+PTX	P= >0.999	P= 0.922

Mean ± Standard Deviation. One-way ANOVA followed by Tukey's post comparison test to compare mean of each group to all other groups. A bolded P value is considered significant ($P<0.05$).

Table 4-2. Cell population percentages for microglia in BXD43 and B6 mice.

Groups	CX_3CR1^- $F4/80^+$ Cells- Percentage of R2	CX_3CR1^+ $F4/80^+$ Cells- Percentage of R2	CX_3CR1^+ $F4/80^-$ Cells- Percentage of R2	CX_3CR1^- $CD206^+$ Cells- Percentage of R2	CX_3CR1^+ $CD206^+$ Cells- Percentage of R2	$CX3CR1^+$ $CD206^-$ Cells- Percentage of R2
BXD43 (Mock)	3.33 ± 1.02	82.4 ± 2.11	2.00 ± 0.53	0.0 ± 0	0.14 ± 0.24	85.7 ± 2.00
BXD43 EAE	25.8 ± 19.9	51.3 ± 31.32	0.31 ± 0.35	1.17 ± 1.18	0.33 ± 0.29	54.6 ± 30.4
B6 (Mock)	1.78 ± 1.01	79.4 ± 6.45	32.9 ± 43.85	0.08 ± 0.14	2.53 ± 1.52	86.0 ± 7.01
B6 EAE	8.76 ± 8.59	74.5 ± 7.3	8.05 ± 1.06	0.39 ± 0.19	4.51 ± 1.95	79.7 ± 4.91
B6 EAE+PTX	29.8 ± 22.8	52.2 ± 26.1	2.88 ± 4.44	0.49 ± 0.80	0.73 ± 0.25	58.8 ± 29.0
All groups	P= 0.518	P= 0.570	**P= 0.0068**	P= 0.263	**P= 0.0034**	P= 0.194
BXD43 (Mock) and B6 (Mock)	P= 0.9961	P= >0.999	P= 0.0668	P= >0.999	P= 0.143	P= >0.999
BXD43 (Mock) and B6 EAE	P= >0.999	P= 0.984	P= 0.216	P= 0.940	**P= 0.0054**	P= 0.995
BXD43 (Mock) and B6 EAE+PTX	P= 0.220	P= 0.344	P= >0.999	P= 0.878	P= 0.065	P= 0.467
BXD43 EAE and B6 (Mock)	P= 0.296	P= 0.409	P= 0.0147	P= 0.306	P= 0.194	P= 0.331
BXD43 EAE and B6 EAE	P= 0.595	P= 0.577	P= 0.0473	P= 0.601	P= 0.0073	P= 0.530
BXD43 EAE and B6 EAE+PTX	P= 0.996	P= >0.999	P= 0.866	P= 0.705	P= 0.991	P= 0.999

Mean ± Standard Deviation. One-way ANOVA followed by Tukey's post comparison test to compare mean of each group to all other groups. A bolded P value is considered significant ($P<0.05$).

Figure 4-4. BXD43 mice with EAE show lower expression of CX_3CR1^+ microglia than healthy BXD43 mice.

(A) Gating strategy for microglia populations. (B) Microglia gated for CX_3CR1 and F4/80 in BXD43 and B6 mice with EAE. The BXD43 mice and B6 EAE+PTX mice were harvested on day 15, whereas the B6 mice and B6 EAE mice were harvested on day 29. (C) Microglia gated for CX_3CR1 and CD206 in BXD43 and B6 mice with EAE.

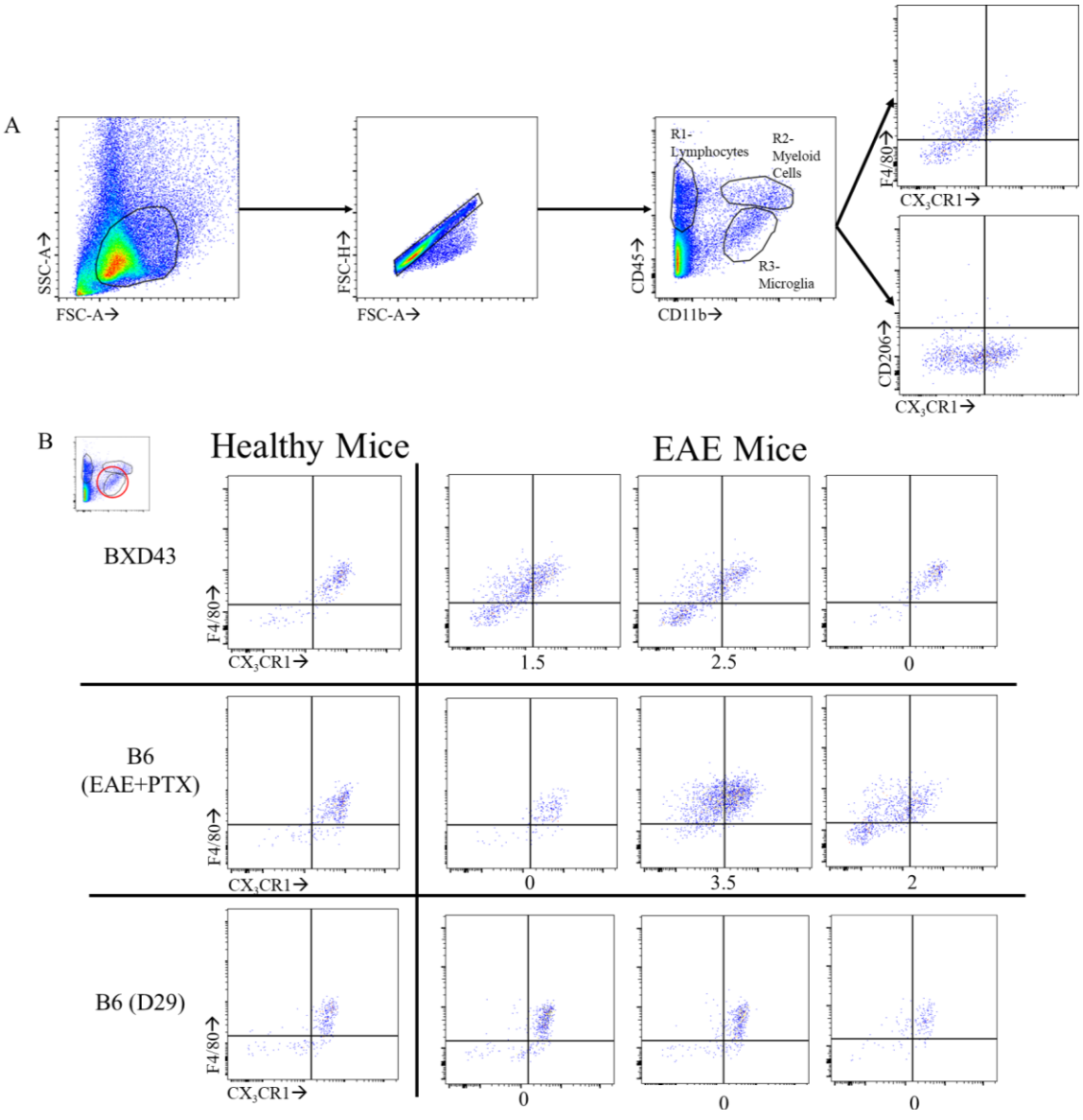
A
SSC-A→
FSC-A→
FSC-H→
FSC-A→
R1-
Lymphocytes
R2-
Myeloid
Cells
R3-
Microglia
CD45→
CD11b→
F4/80→
CX3CR1→
CD206→
CX3CR1→
B
Healthy Mice
EAE Mice
BXD43
B6
(EAE+PTX)
B6 (D29)
F4/80→
CX3CR1→
1.5
2.5
0
0
3.5
2
0
0
0

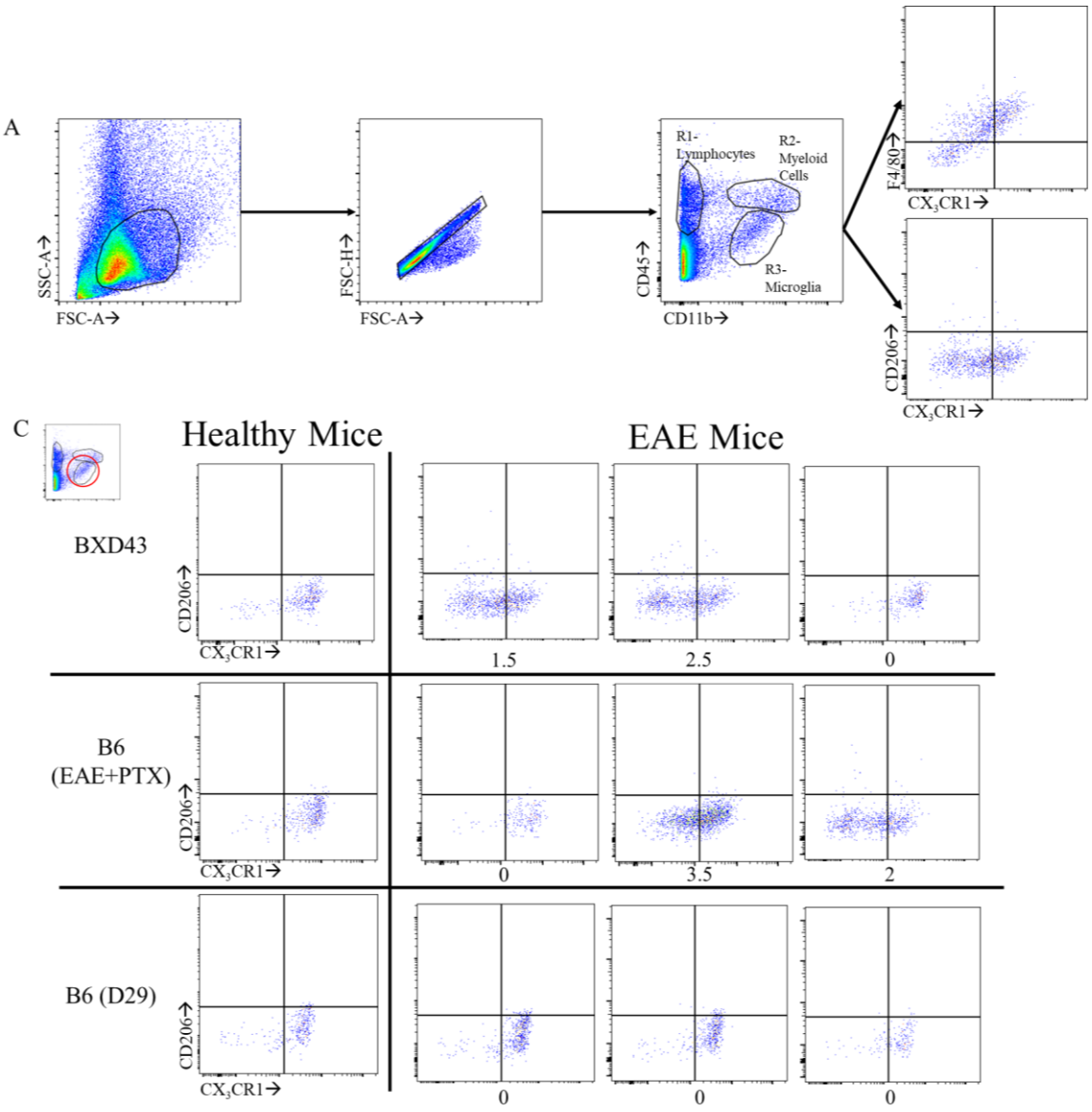

Figure 4-4. Continued.

Figure 4-5. BXD43 mice with EAE and B6 mice with EAE+PTX show a greater population of Ly6C$^+$ monocytes than healthy mice.

(A) Gating strategy for myeloid cells in BXD43 and B6 spinal cord samples. (B) Myeloid cells in BXD43 and B6 mice with EAE gated for Ly6C and MHC Class II to identify activated monocytes. (C) Myeloid cells in BXD43 and B6 mice gated for Ly6C and CD80 to identify activated monocytes.

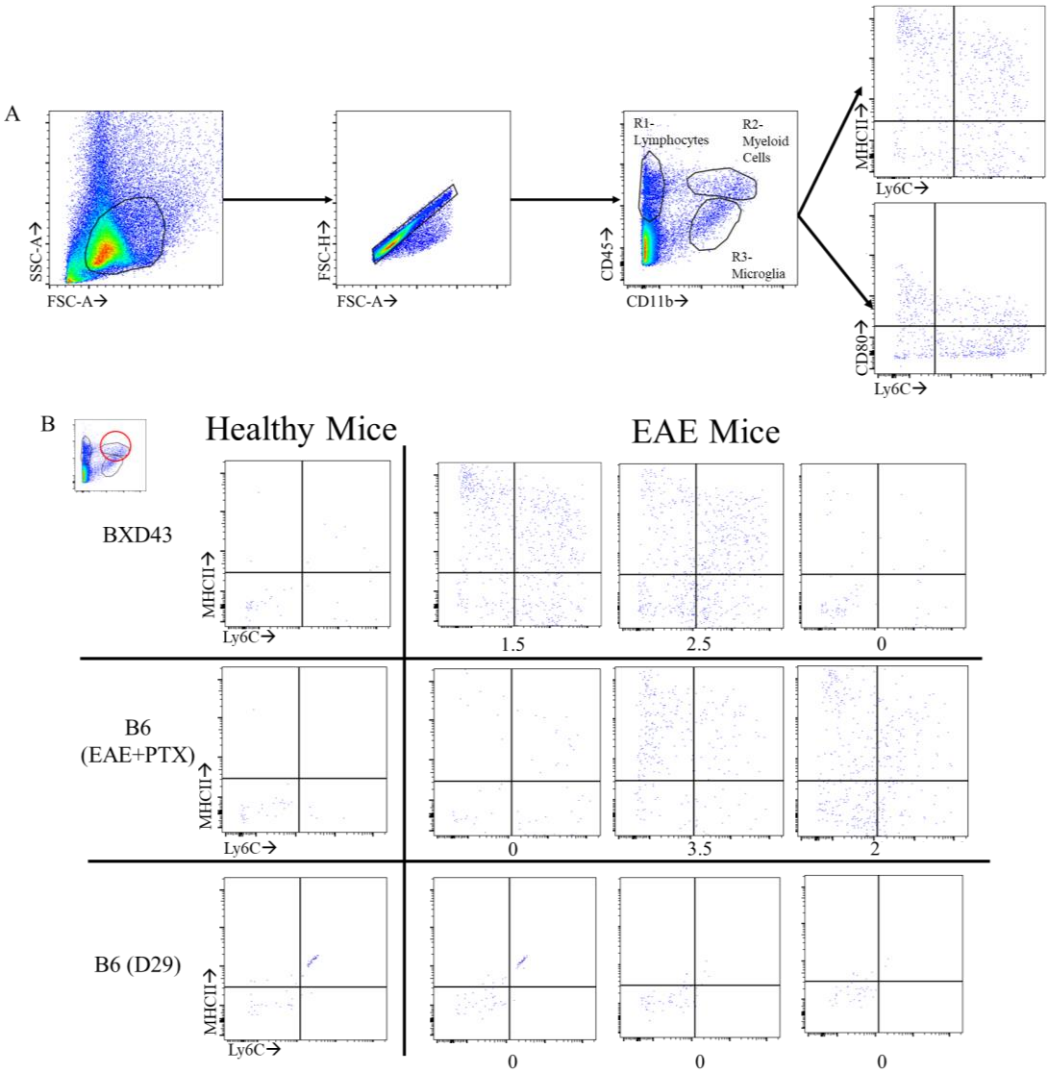
A
SSC-A→
FSC-A→
FSC-H→
FSC-A→
R1-
Lymphocytes
R2-
Myeloid
Cells
R3-
Microglia
CD45→
CD11b→
MHCII→
Ly6C→
CD80→
Ly6C→
B
Healthy Mice
EAE Mice
BXD43
B6
(EAE+PTX)
B6 (D29)
MHCII→
Ly6C→
1.5
2.5
0
0
3.5
2
0
0
0

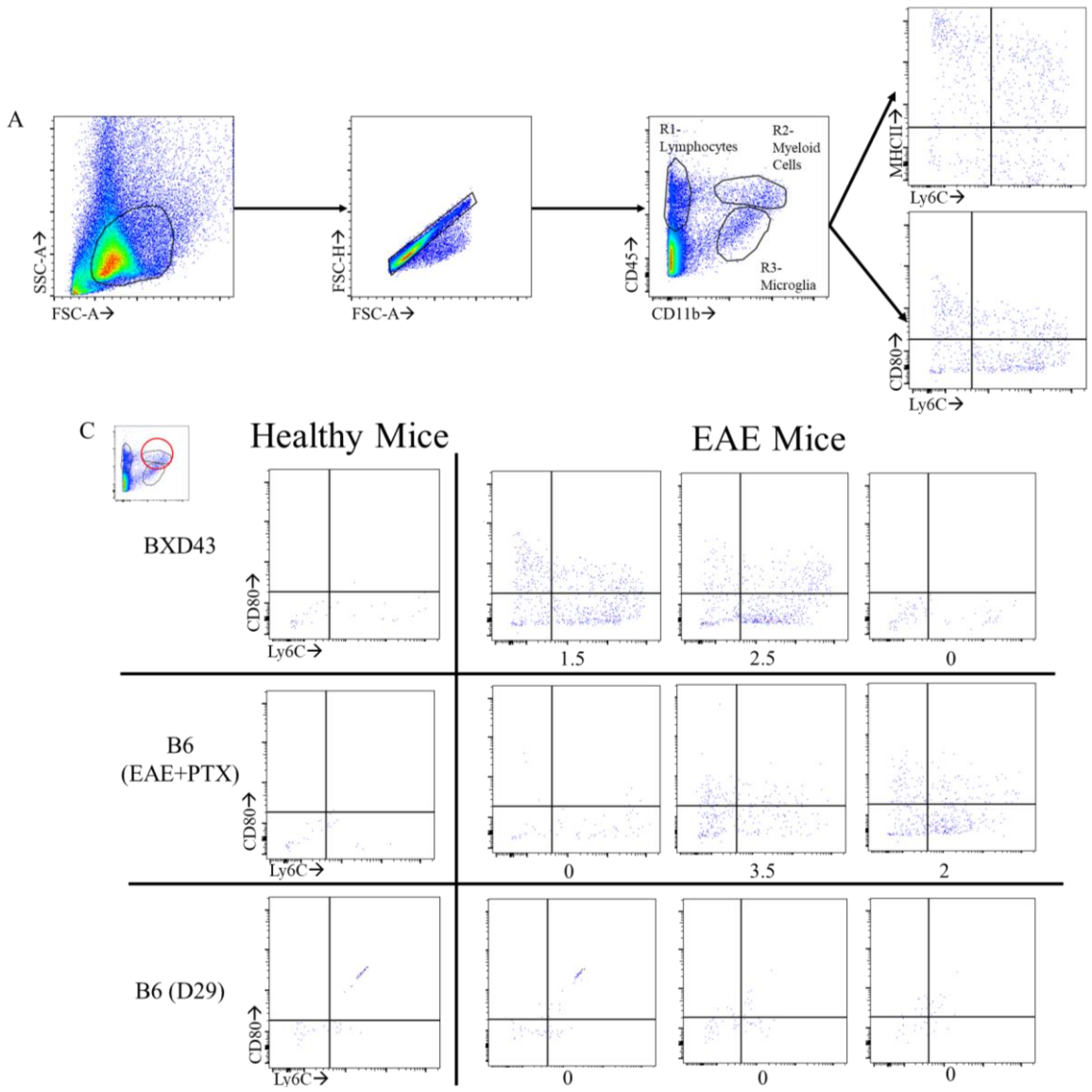

Figure 4-5. Continued.

determined to be significant. (**Figure 4-5B** and **C**). Additionally, the BXD43 mice with EAE showed a trend towards a higher number of $MHCII^+$ monocytes, suggesting that these monocytes may also show more activation, and thus may be more damaging to the CNS (**Table 4-3**)

Changes in Lymphocyte Populations of BXD43 Mice

We used the following gating strategy to identify lymphocytes that had infiltrated the spinal cord of MOG immunized mice. Cells were identified as described in **Table 2-6**. First, the cells were first gated to exclude doublets, and then gated for TCRβ vs CD19 to separate T cells ($TCR\beta^+$) and B cells ($CD19^+$) (**Figure 4-6B** and **C**). Next, the T cells were gated for $CD8^+$ cells and $CD4^+$ cells to separate out the cytotoxic T cell population and the helper T cell population, respectively (**Figure 4-6C**).

After gating, we compared the total cell count for the lymphoid cell populations for the spinal cell samples in the BXD43 and B6 mice with EAE. In both the BXD43 and B6 strains with EAE, there was an increase in lymphocytes, suggesting an increase in lymphocytes migrating to the spinal cord, though not enough to be considered significant (**Figure 4-6B and D**). There was no significant difference between the BXD43 EAE mice and the B6 EAE+PTX mice (**Table 4-4**).

Based on these results, the BXD43 EAE mice showed a greater similarity in immune cell populations to the B6 EAE+PTX mice, with a trend of increases in microglia, inflammatory monocytes, and lymphocytes compared to the BXD43 Control group. However, we did not find a significant difference between the BXD43 EAE mice and the B6 EAE+PTX for any of the immune cell populations. It is noteworthy that the BXD43 mice reached this level of immune cell infiltration and severity without the need for a PTX dose to increase incidence rate. This is seen when comparing the values of the BXD43 EAE mice and the B6 EAE groups (**Table 4-4**). Future studies would benefit from measuring immune cell infiltrates at other time points, rather than at the peak clinical score. This may give more insight into the changes in migration of the cells.

Changes in Cytokine and Chemokine Levels in BXD43 Mice with EAE

To determine if there were changes in inflammatory cytokines and chemokines in the serum of BXD43 and B6 mice immunized with MOG, we performed a multiplex immunoassay. Serum samples were taken from BXD43 and B6 mice with EAE or healthy controls at various time points to determine changes both at the beginning of EAE and at the peak disease severity. The serum from healthy controls were treated as day 0 for the analysis.

Table 4-3. Cell population percentages for myeloid cells in BXD43 and B6 mice.

Groups	Ly6C$^-$ MHCII$^+$ Cells-Percentage of R3	Ly6C$^+$MHC II$^+$ Cells-Percentage of R3	Ly6C$^+$MHC II$^-$ Cells-Percentage of R3	Ly6C$^-$ CD80+ Cells-Percentage of R3	Ly6C$^+$CD80$^+$ Cells-Percentage of R3	Ly6C$^+$CD80$^-$ Cells-Percentage of R3
BXD43 (Mock)	11.62 ± 6.65	15.2 ± 8.53	20.3 ± 3.56	1.71 ± 2.96	3.34 ± 3.94	42.9 ± 9.83
BXD43 EAE	23.8 ± 12.2	28.6 ± 14.9	17.57 ± 0.93	9.29 ± 10.26	13.77 ± 11.92	43.8 ± 10.48
B6 (Mock)	9.9 ± 8.89	24.2 ± 33.6	8.29 ± 4.89	1.11 ± 1.92	23.42 ± 20.35	28.07 ± 13.2
B6 EAE	8.97 ± 4.99	19.6 ± 23.79	2.66 ± 3.62	13.3 ± 10.47	33.3 ± 20.35	17.5 ± 9.9
B6 EAE+PTX	36.20 ± 24.2	23.70 ± 3.18	17.49 ± 13.10	14.13 ± 8.12	12.4 ± 5.10	43.57 ± 17.45
All groups	P= 0.126	P= 0.0720	**P= 0.04**	P= 0.175	P= 0.417	P= 0.09
BXD43 (Mock) and B6 (Mock)	P= >0.999	P= 0.979	P= 0.252	P= >0.999	P= 0.705	P= 0.610
BXD43 (Mock) and B6 EAE	P= 0.999	P= 0.999	P= 0.054	P= 0.398	P= 0.366	P= 0.169
BXD43 (Mock) and B6 EAE+PTX	P= 0.233	P= 0.983	P= 0.984	P= 0.338	P= 0.975	P= >0.999
BXD43 EAE and B6 (Mock)	P= 0.713	P= 0.979	P= 0.473	P= 0.693	P= 0.969	P= 0.562
BXD43 EAE and B6 EAE	P= 0.661	P= 0.998	P= 0.117	P= 0.964	P= 0.723	P= 0.150
BXD43 EAE and B6 EAE+PTX	P= 0.782	P= 0.998	P= >0.999	P= 0.933	P= >0.999	P= >0.999

Mean ± Standard Deviation. One-way ANOVA followed by Tukey's post comparison test to compare mean of each group to all other groups. A bolded P value is considered significant ($P<0.05$).

Figure 4-6. BXD43 mice with EAE and B6 mice with EAE+PTX show a higher population of $CD4^+$ T cells than healthy mice.

(A) Gating strategy for identifying lymphocyte populations in spinal cord samples from BXD43 and B6 mice with EAE. (B) Lymphocytes in BXD43 and B6 mice with EAE gated for TCRβ to identify T cell populations. (C) T cells in BXD43 and B6 mice with EAE gated for CD4 and CD8 to identify helper T cells and cytotoxic T cells, respectively. (D) Lymphocytes in BXD43 and B6 mice with EAE gated for CD19 to identify B cell populations.

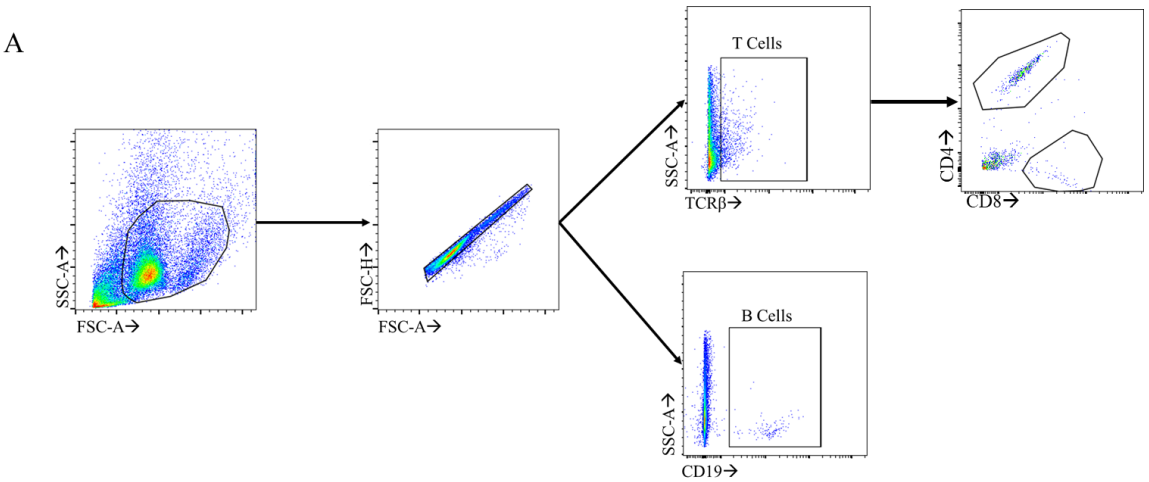
A
SSC-A→
FSC-A→
FSC-H→
FSC-A→
T Cells
SSC-A→
TCRβ→
CD4→
CD8→
B Cells
SSC-A→
CD19→

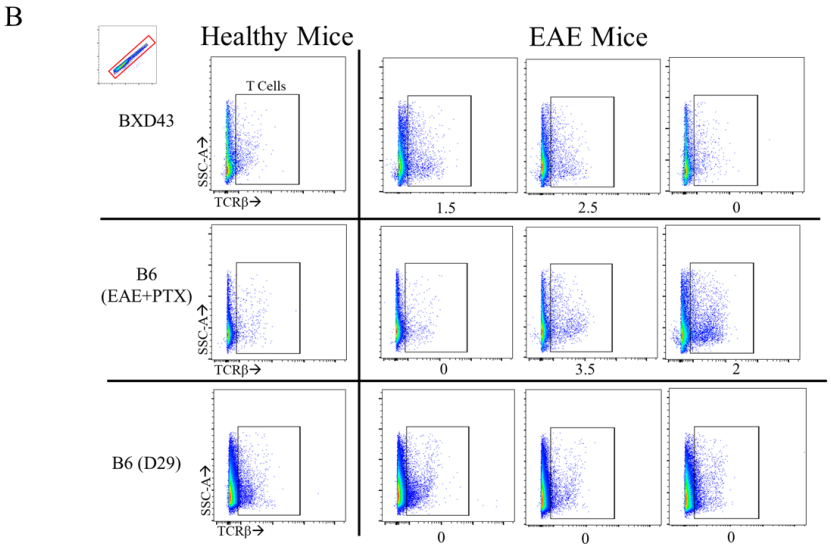
B
Healthy Mice
EAE Mice
T Cells
BXD43
SSC-A→
TCRβ→
1.5
2.5
0
B6
(EAE+PTX)
0
3.5
2
B6 (D29)
0
0
0

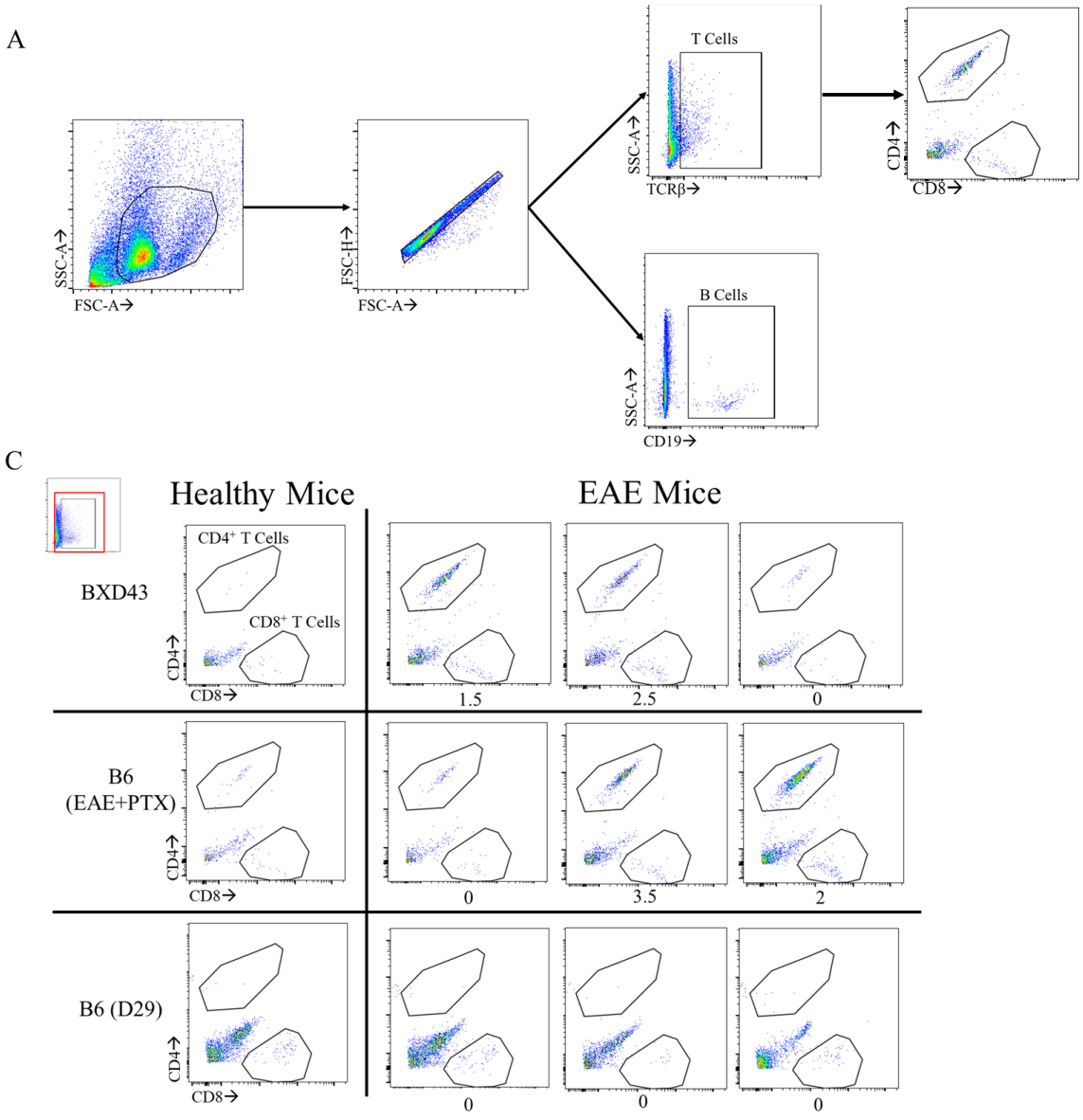

Figure 4-6. Continued.

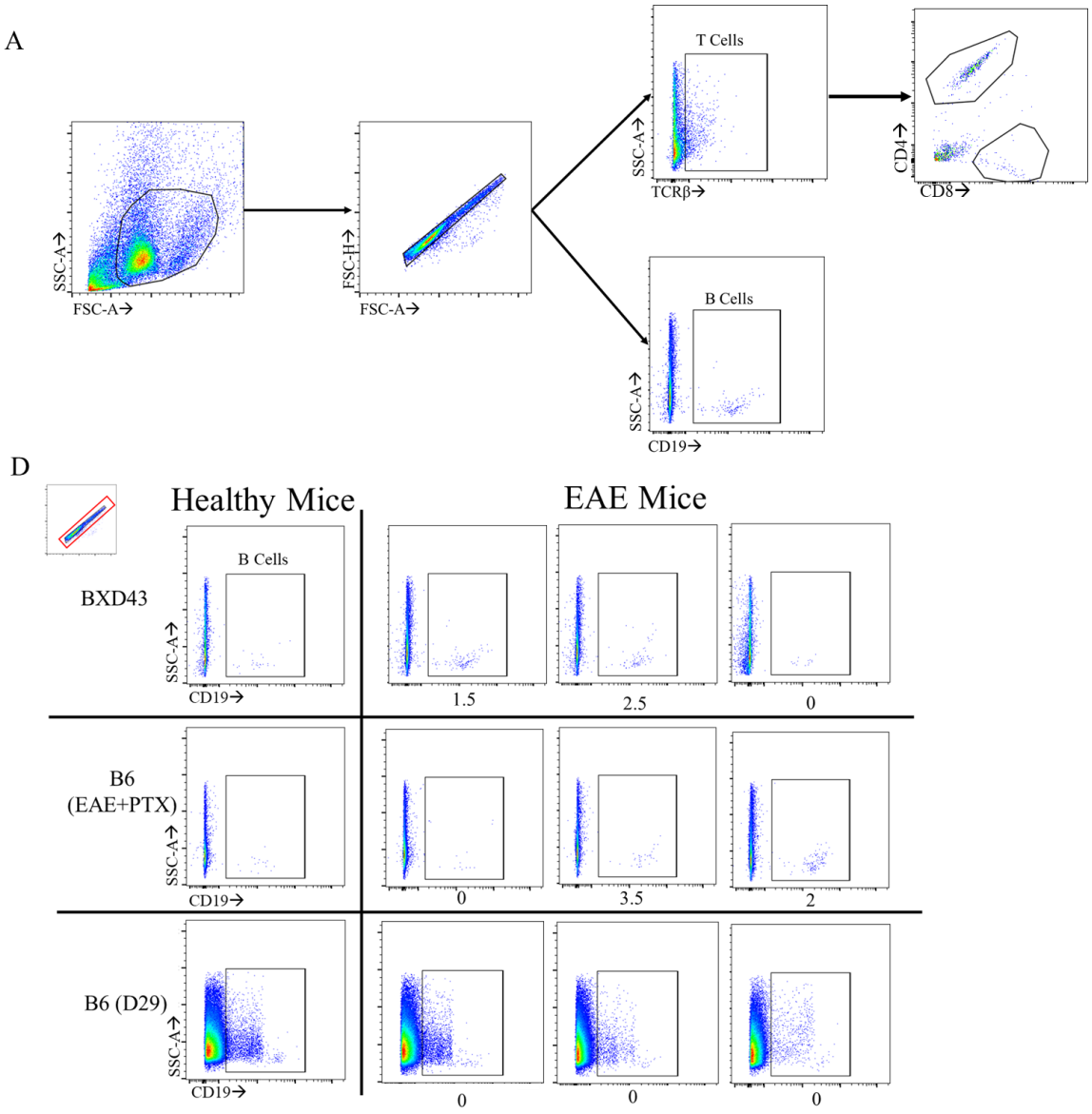

Figure 4-6. Continued.

Table 4-4. BXD43 mice with EAE show higher populations of $CD4^+$ and $CD8^+$ T cells in the spinal cord.

Groups	B Cells	T Cells	$CD4^+$ T Cells- Percentage of T Cells	$CD8^+$ T Cells- Percentage of T Cells
BXD43 (Mock)	0.16 ± 0.09	3.62 ± 2.62	0.07 ± 0.06	0.14 ± 0.11
BXD43 EAE	0.3 ± 0.15	4.48 ± 0.46	1.19 ± 0.73	0.19 ± 0.08
B6 (Mock)	1.08 ± 1.77	1.99 ± 1.06	0.09 ± 0.08	0.06 ± 0.03
B6 EAE	1.65 ± 0.91	3.36 ± 1.46	0.01 ± 0.01	0.06 ± 0.04
B6 EAE+PTX	0.19 ± 0.16	5.27 ± 3.41	2.45 ± 2.25	0.19 ± 0.12
All groups	P= 0.244	P= 0.431	**P= 0.013**	P= 0.480
BXD43 (Mock) and B6 (Mock)	P= 0.724	P= 0.870	P= 0.995	P= 0.999
BXD43 (Mock) and B6 EAE	P= 0.319	P= >0.999	P= 0.999	P= 0.757
BXD43 (Mock) and B6 EAE+PTX	P= >0.999	P= 0.864	**P= 0.0364**	P= 0.998
BXD43 EAE and B6 (Mock)	P= 0.824	P= 0.610	P= 0.303	P= 0.844
BXD43 EAE and B6 EAE	P= 0.407	P= 0.962	P= 0.124	P= 0.343
BXD43 EAE and B6 EAE+PTX	P= >0.999	P= 0.989	P= 0.825	P= 0.988

Mean ± Standard Deviation. One-way ANOVA followed by Tukey's post comparison test to compare mean of each group to all other groups. A bolded P value is considered significant ($P<0.05$).

We collected serum from BXD43 and B6 mice at day 0 (no EAE injection) and day 1 post injection to determine if any cytokine and chemokine levels would change after 24 hours. The BXD43 mice showed a higher level of IL-12p70 on day 0. Both B6 and BXD43 showed a slight increase in the following on day 1: IL-1β, IL-6, MCP-3, and eotaxin. B6 mice showed elevated levels of IL-4, IL-22, GROα, and IL-17A (**Figure 4-7**). Additionally, the following cytokines and chemokines were found to not have any notable changes between the groups: GM-CSF, IL-10, IL-2, IL-27, IFNγ, IL-5, IL-9, IL-13, MIP-1α, IL-18, and MIP-1β. However, the only change that was determined to be statistically significant was found to be MIP-2a, with a significant increase of MIP-2a in the BXD43 mice. Based on these changes, in both B6 and BXD43 mice, there is a trend towards an increase in inflammatory cytokines and chemokines 24 hours post injection. At the average day of peak EAE, BXD43 mice showed a significant increase in IP-10, RANTES, MIP-2a, and TNF-α **(Figure 4-7).** IP-10 serves as a chemoattractant for inflammatory cells such as T_H1 cells, NK cells, and B cells. RANTES is associated with promoting inflammation by attracting cells such as monocytes, macrophages, T_H1 cells, NK cells, basophils, and eosinophils. MIP-2a also serves to promote inflammation by attracting monocytes, macrophages, T_H1 cells, NK cells, basophils, and dendritic cells. Finally, TNF-α promotes inflammation via T cell signaling and promotes inflammatory T_H17 differentiation [58]. Surprisingly, BXD43 mice with EAE on day 1 did not show elevated levels of IL-17A, which is associated with EAE pathology. Similarly, there was no increase in GROa, a chemoattractant for neutrophils (**Figure 4-7**).

The increase in these inflammatory markers in the serum of BXD43 mice further indicates that there is a high level of inflammation in the spinal cords of BXD43 mice with EAE, which may result in a much more rapid degradation of myelin in the spinal cord.

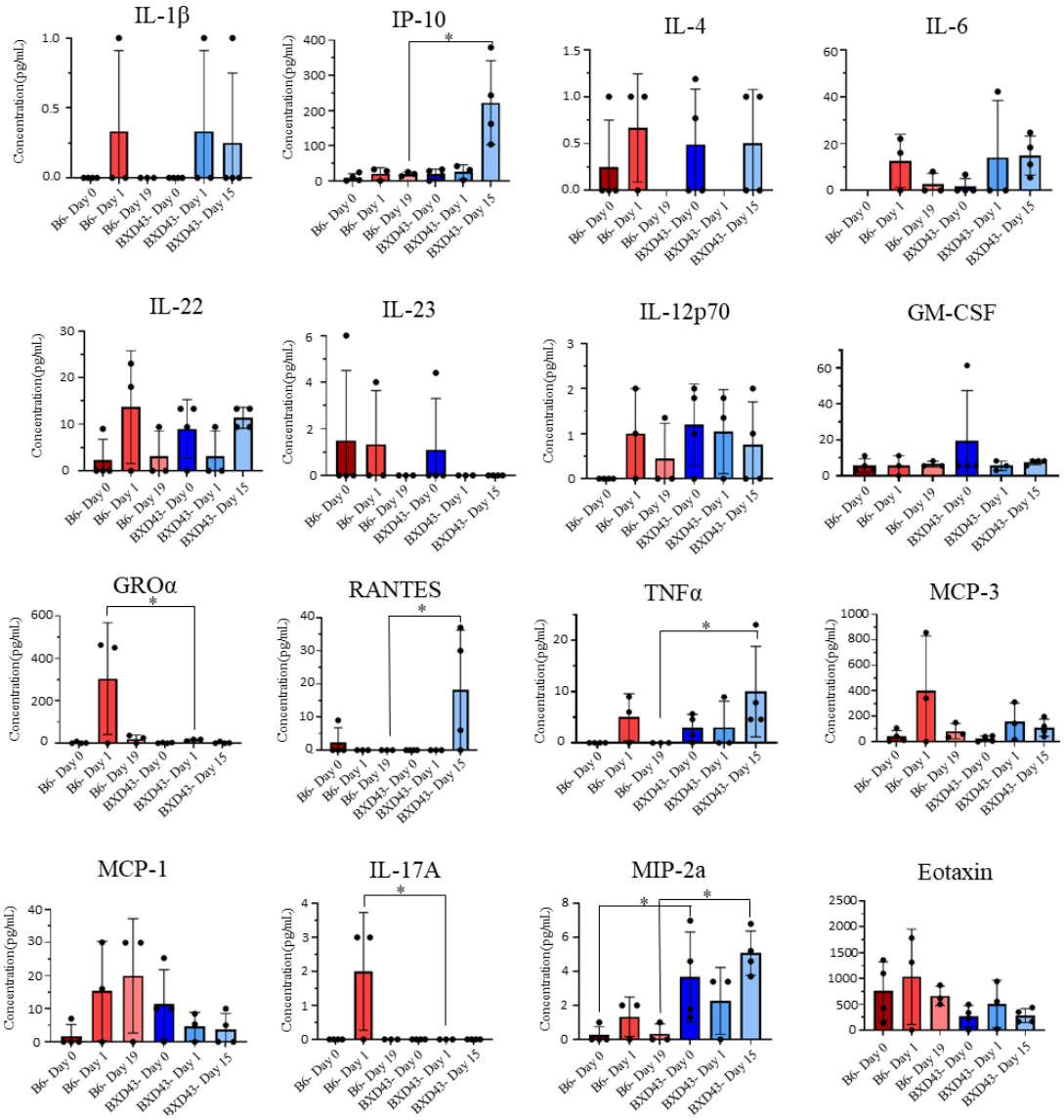

Figure 4-7. BXD43 and B6 mice show differing inflammatory cytokine and chemokine levels at day 0, day 1, and day of average peak EAE score.

Comparison of cytokine and chemokine levels of serum samples in BXD43 and B6 mice with EAE at day 0 (Control), day 1, and day 15 for the BXD43 mice and day 19 for B6 mice. Cytokines and chemokines were measured at pg/mL. One-way ANOVA followed by Tukey's post comparison test to compare mean of each group to the other strain of the equivalent day. Asterisk (*) marks a change considered significant (P=<0.05)

CHAPTER 5. DISCUSSION

The purpose of this research was to first determine which BXD strains were susceptible to EAE, and from there utilize GeneNetwork to map out potential QTLs associated with EAE susceptibility and severity using data from all BXD strains tested. However, after determining that the BXD43 strain was not only susceptible to EAE, but that it also developed extremely rapid and severe EAE, we also investigated the differences between the BXD43 mice and B6 mice when induced with EAE.

BXD Strains Show a Spectrum of EAE Susceptibility

Our induction studies showed a great level of variety in EAE susceptibility in the BXD mouse family. Out of 16 strains, only 6 showed EAE symptoms after 30 days post immunization, and only a single strain expressed a score higher than a 1.5 (**Figure 3-2A**). These results reflect what has been seen with previous EAE models in that it can be difficult to induce EAE in mice depending on the strain and myelin peptide used. This is seen in the parent strain B6, which in these studies only showed an incidence rate of 43% without a PTX treatment (**Figure 3-3A**). The results of these studies allowed us to map possible QTLs associated with final clinical score, incidence rate of EAE, length of acute onset, and peak score (**Figure 3-4**). The results suggests that chromosomes 5 and 11 may contain loci related these traits.

For final clinical score, peak clinical score, incidence rate, and length of acute onset (or length of time the mouse is showing symptoms), the potential QTL on chromosome 5 was found to be at the same spot at 45.25 megabases. The only identifiable gene near this region, according to GeneNetwork, is *QDPR*, which codes for the enzyme dihydropteridine reductase, while other segments of DNA in the region have been mapped but their function is currently unknown. Dihydropteridine reductase is involved in folate synthesis in the brain, though its relevance in EAE or MS is currently unknown [59] A recent study did not see any difference in folate levels in patients with RRMS than with healthy controls, so more research is needed to determine if folate plays a role in EAE or MS [60]. Based on these results, it may be worthwhile to further investigate the role of folate synthesis and the development of EAE and MS. It may also be that the gene for this region has not yet been identified. Additionally, there was also a potential QTL for final clinical score on chromosome 17, but there were no relevant genes in the region. This suggests that a potentially relevant gene has not yet been identified.

The final potential QTL for length of acute onset was found on chromosome 11, between 64.5-67.5 megabases. There are several identified genes in this region, including several genes for myosin and heparan sulfate. However, one gene stood out for its potential role in immune regulation: *MAP2K4*. This gene codes for the enzyme that phosphorylates MAP kinases. Previous studies have shown how MAPK function is linked to T cell development and immune response to viral infections [61]. Additionally,

activation of c-Jun NH2-terminal kinases (JNKs), a type of MAPK, have been shown to be associated with the release of several proinflammatory cytokines such as GM-CSF, RANTES, and IL-8, further suggesting a prominent role in immunoregulation [62]. This suggests a promising gene directly linked to immune function could be associated with length of acute onset, and that variations in this gene may account for some BXD strains developing EAE symptoms at earlier dates than others.

Due to the small sample size and relatively small number of strains tested, all possible QTLs mapped were only found to be considered suggestive, rather than significant. Increasing the number of BXD strains tested will help improve the specificity and accuracy of the calculation. However, these studies demonstrate how the BXD family is an extremely useful tool in determining genetic loci associated with disease outcome. One notable limitation of these induction studies is duration of disease, as all studies were ended at 30 days. Future studies with the BXD strains that are susceptible to EAE may benefit from extending past 30 days, to determine if symptoms worsen or improve with time.

BXD43 as an Extreme Phenotype

The BXD43 strain was found to be extremely susceptible to EAE, showing a fast disease progression and severe EAE symptoms. From these initial studies, the strain seemed promising as a potential model for severe EAE, as mice showed a continuous increase in disease severity until reaching the humane endpoint. Additionally, the mice showed severe EAE development without the need for a PTX injection to increase incidence rate, unlike the B6 model that only shows an incidence rate of 43% without PTX. (**Table 3-1**). Studies have shown that PTX helps to suppress the Treg response in mice immunized with CFA/MOG_{35-55} to induce EAE [63]. As the BXD43 mice did not need this additional help to induce EAE, it may suggest the BXD43 mice show a differing immune response than the B6, and thus would allow the BXD43 mouse to provide a new model for EAE.

To better characterize the differences between the BXD43 and B6 model, we investigated changes in immune cell populations and changes in cytokines and chemokines. The results showed a significant increase in inflammatory monocytes in the BXD43 mice with EAE when compared to healthy BXD43 mice (**Table 4-3**). These proinflammatory monocytes have been found to be essential to the pathogenesis of EAE via infiltration of CNS [64]. This large amount of inflammatory monocyte migration into the CNS may promote inflammation and neurodegeneration through the secretion of CCL2, a chemoattractant secreted by monocytes and macrophages that attracts several immune cells essential to the pathogenesis of EAE, including T cells, monocytes, dendritic cells, and neutrophils [45]. Previous studies have shown that the secretion of CCL2 is essential for EAE development in mice, and thus an increase in this cytokine may lead to increased cell migration to the CNS [42]. However, the results showed that there was no significant difference between the inflammatory monocytes of the BXD43 mice with EAE and the B6 mice with EAE+PTX.

We also saw that when comparing the BXD43 mice with EAE and the B6 mice with EAE+PTX, there was a higher percentage of $CD4^+$ T cells in the spinal cord, though not high enough to be considered statistically significant (**Table 4-4**). This may be due to a low sample number, as there were only 3 mice per group in this study, and one mouse did not show any EAE symptoms. $CD4^+$ T cells play an essential role in EAE pathogenesis by the release of proinflammatory cytokines that promote the recruitment of other proinflammatory cells. As reviewed in Krishnarajah, S. et al, 2022, T_H1 cells release IFNγ and GM-CSF, which leads to the activation of resident microglia and differentiation of DCs, respectively [65]. T_H17 cells produce IL-17, a cytokine that creates a positive feedback loop in EAE by promoting IL-1β, which in turn promotes T_H17 cell survival and proliferation in the CNS [49]. IL-17 is a proinflammatory cytokine that induced the production of other cytokines by triggering several signal cascades [49] An increase in the concentration of these helper T cell subsets in the CNS leads to more severe EAE [66]. One notable T cell population we did not look at was Tregs, which can mitigate EAE severity in mice [50]. Several studies have shown that the ratio of T_H1/Treg cells and T_H17/Treg cells affects EAE severity, as Treg cells can suppress the pathogenic activities of T_H1 and T_H17 cells by regulating cytokine signaling [50, 67, 68]. As reviewed by Bar-Or et al, 2021, the balance between Tregs and T_H1 and T_H17 cells also plays an equivalent role in regulating MS [69]. Quantifying Treg numbers in BXD43 mice with EAE would be beneficial to determine if a change in the T_H1/T_H17/Treg ratio may be the cause of the severe EAE seen in the BXD43 mouse.

We also saw differing cytokine and chemokine levels in serum samples from BXD43 and B6 mice with EAE. Several inflammatory cytokines and chemokines were found to be elevated in the BXD43 mice, at day 0, day 1, and day 15, such as IP-10, RANTES, and TNFα (**Figure 4-7**). IP-10, also known as CXCL10, is a chemokine that is produced by monocytes and neutrophils that serves as a chemoattractant for T cells and NK cells to inflamed tissues [70] An increase in IP-10 expression has been shown to increase migration of cells to inflamed areas of the CNS [71]. RANTES, also known as CCL5, is a chemokine produced by T cells and monocytes, and serves as a chemoattractant for cells such as T cells, monocytes, macrophages, and T cells, and NK cells [72] Reduction of RANTES has also been shown to delay development of EAE in mice [73]. TNF-α is a cytokine produced by macrophages, NK cells, and T cells, and promotes inflammation by promoting production of several other inflammatory cytokines. Increases in TNF-α production in EAE mice have been shown to impair Treg function, increasing EAE severity, while blocking TNF-α has reduced disease severity [74]. All three of these cytokines and chemokines are directly involved in either promoting migration of inflammatory cells or production of other inflammatory cytokines. The increase in these proinflammatory cytokines and chemokines is likely a factor in why the BXD43 mice show significantly higher inflammatory monocytes in the CNS, as well as rapid EAE development.

However, it was notable that we did not see an increase in IL-17a, which is secreted by T_H17 cells and as stated earlier, is a cytokine involved in signal cascades of other proinflammatory cytokines [49]. It works in concert with other cytokines such as TNF-α and has been shown to be crucial in the development of EAE [49]. It is possible

that we did not see an increase in IL-17 in the serum but may see an increase in the CFS of the BXD43 mice with EAE. Future studies would benefit from measuring cytokine and chemokine levels both in the serum and in the CSF.

Conclusions

The two primary conclusions for these studies are that the BXD family of mice may be utilized to determine potential QTLs for EAE susceptibility, and that the BXD43 strain can serve as an effective mouse model for rapid and severe EAE. Using the GeneNetwork database, we found that there are potential QTLs for incidence rate of EAE, final clinical score, length of acute onset, and peak clinical score on chromosomes 5, 11, and 17. Two genes near those potential QTLs, *QDPR* and *MAPK2K4*, may be linked to EAE development, and thus their human analogues may also be linked to susceptibility to MS. Further research with more BXD strains is needed to further clarify these gene candidates. We also found that the BXD43 strain can serve as an invaluable model that better reflects rapid EAE, allowing for more effective research into potential treatments, showing a similar disease profile to the B6 EAE model with PTX. As there are currently few effective treatments for PPMS, there is a great need for diverse EAE models to help find new therapeutic targets. The expansion of research opportunities, both in genetics and animal models, will help further the field of the treatment and prevention of MS, as well as other neurodegenerative diseases of the CNS.

LIST OF REFERENCES

1. Reich, D. S., Lucchinetti, C. F., & Calabresi, P. A. (2018). Multiple Sclerosis. New England Journal of Medicine, 378(2), 169-180. https://doi.org/10.1056/nejmra1401483

2. Lane, J., Ng, H. S., Poyser, C., Lucas, R. M., & Tremlett, H. (2022). Multiple sclerosis incidence: A systematic review of change over time by geographical region. Multiple Sclerosis and Related Disorders, 63, 103932. https://doi.org/10.1016/j.msard.2022.103932

3. Compston, A., & Coles, A. (2008). Multiple sclerosis. The Lancet, 372(9648), 1502-1517. https://doi.org/https://doi.org/10.1016/S0140-6736(08)61620-7

4. Frischer, J. M., Bramow, S., Dal-Bianco, A., Lucchinetti, C. F., Rauschka, H., Schmidbauer, M., Laursen, H., Sorensen, P. S., & Lassmann, H. (2009). The relation between inflammation and neurodegeneration in multiple sclerosis brains. Brain, 132(Pt 5), 1175-1189. https://doi.org/10.1093/brain/awp070

5. Dendrou, C. A., Fugger, L., & Friese, M. A. (2015). Immunopathology of multiple sclerosis. *Nature Reviews Immunology*, *15*(9), 545-558. https://doi.org/10.1038/nri3871

6. Lunde, H. M. B., Assmus, J., Myhr, K.-M., Bø, L., & Grytten, N. (2017). Survival and cause of death in multiple sclerosis: a 60-year longitudinal population study. Journal of Neurology, Neurosurgery & Psychiatry, 88(8), 621-625. https://doi.org/10.1136/jnnp-2016-315238

7. McGinley, M. P., Goldschmidt, C. H., & Rae-Grant, A. D. (2021). Diagnosis and Treatment of Multiple Sclerosis. JAMA, 325(8), 765. https://doi.org/10.1001/jama.2020.26858

8. Martínez-Heras, E., Solana, E., Prados, F., Andorrà, M., Solanes, A., López-Soley, E., Montejo, C., Pulido-Valdeolivas, I., Alba-Arbalat, S., Sola-Valls, N., Sepúlveda, M., Blanco, Y., Saiz, A., Radua, J., & Llufriu, S. (2020). Characterization of multiple sclerosis lesions with distinct clinical correlates through quantitative diffusion MRI. Neuroimage Clin, 28, 102411. https://doi.org/10.1016/j.nicl.2020.102411

9. Bar-Or, A., & Li, R. (2021). Cellular immunology of relapsing multiple sclerosis: interactions, checks, and balances. The Lancet. Neurology, 20(6), 470–483. https://doi.org/10.1016/S1474-4422(21)00063-6

10. Moser, T., Akgün, K., Proschmann, U., Sellner, J., & Ziemssen, T. (2020). The role of TH17 cells in multiple sclerosis: Therapeutic implications. Autoimmun Rev, 19(10), 102647. https://doi.org/10.1016/j.autrev.2020.102647

11. Frisullo, G., Nociti, V., Iorio, R., Patanella, A. K., Caggiula, M., Marti, A., Sancricca, C., Angelucci, F., Mirabella, M., Tonali, P. A., & Batocchi, A. P. (2009). Regulatory T cells fail to suppress CD4T+-bet+ T cells in relapsing multiple sclerosis patients. Immunology, 127(3), 418–428. https://doi.org/10.1111/j.1365-2567.2008.02963.x

12. McKay, F. C., Swain, L. I., Schibeci, S. D., Rubio, J. P., Kilpatrick, T. J., Heard, R. N., Stewart, G. J., & Booth, D. R. (2008). CD127 immunophenotyping suggests altered CD4+ T cell regulation in primary progressive multiple sclerosis. J Autoimmun, 31(1), 52-58. https://doi.org/10.1016/j.jaut.2008.02.003

13. Zrzavy, T., Hametner, S., Wimmer, I., Butovsky, O., Weiner, H. L., & Lassmann, H. (2017). Loss of 'homeostatic' microglia and patterns of their activation in active multiple sclerosis. Brain, 140(7), 1900-1913. https://doi.org/10.1093/brain/awx113

14. Carstensen, M., Christensen, T., Stilund, M., Møller, H. J., Petersen, E. L., & Petersen, T. (2020). Activated monocytes and markers of inflammation in newly diagnosed multiple sclerosis. Immunology and cell biology, 98(7), 549–562. https://doi.org/10.1111/imcb.12337

15. Comi, G., Bar-Or, A., Lassmann, H., Uccelli, A., Hartung, H. P., Montalban, X., Sørensen, P. S., Hohlfeld, R., & Hauser, S. L. (2021). Role of B Cells in Multiple Sclerosis and Related Disorders. Ann Neurol, 89(1), 13-23. https://doi.org/10.1002/ana.25927

16. Hedström, A. K., Bäärnhielm, M., Olsson, T., & Alfredsson, L. (2011). Exposure to environmental tobacco smoke is associated with increased risk for multiple sclerosis. Mult Scler, 17(7), 788-793. https://doi.org/10.1177/1352458511399610

17. Briggs, F. B., Gunzler, D. D., Ontaneda, D., & Marrie, R. A. (2017). Smokers with MS have greater decrements in quality of life and disability than non-smokers. Multiple Sclerosis Journal, 23(13), 1772-1781. https://doi.org/10.1177/1352458516685169

18. Milo, R., & Kahana, E. (2010). Multiple sclerosis: geoepidemiology, genetics and the environment. Autoimmun Rev, 9(5), A387-394. https://doi.org/10.1016/j.autrev.2009.11.010

19. Miclea, A., Bagnoud, M., Chan, A., & Hoepner, R. (2020). A Brief Review of the Effects of Vitamin D on Multiple Sclerosis. Front Immunol, 11, 781. https://doi.org/10.3389/fimmu.2020.00781

20. Bjornevik, K., Cortese, M., Healy, B. C., Kuhle, J., Mina, M. J., Leng, Y., Elledge, S. J., Niebuhr, D. W., Scher, A. I., Munger, K. L., & Ascherio, A. (2022). Longitudinal analysis reveals high prevalence of Epstein-Barr virus associated with multiple sclerosis. Science, 375(6578), 296-301. https://doi.org/10.1126/science.abj8222

21. Soldan, S. S., & Lieberman, P. M. (2023). Epstein–Barr virus and multiple sclerosis. Nature Reviews Microbiology, 21(1), 51-64. https://doi.org/10.1038/s41579-022-00770-5

22. Sawcer, S., Hellenthal, G., Pirinen, M., Spencer, C. C., Patsopoulos, N. A., Moutsianas, L., Dilthey, A., Su, Z., Freeman, C., Hunt, S. E., Edkins, S., Gray, E., Booth, D. R., Potter, S. C., Goris, A., Band, G., Oturai, A. B., Strange, A., Saarela, J., . . . Compston, A. (2011). Genetic risk and a primary role for cell-mediated immune mechanisms in multiple sclerosis. Nature, 476(7359), 214-219. https://doi.org/10.1038/nature10251

23. Alcina, A., Abad-Grau, M.delM., Fedetz, M., Izquierdo, G., Lucas, M., Fernández, O., Ndagire, D., Catalá-Rabasa, A., Ruiz, A., Gayán, J., Delgado, C., Arnal, C., & Matesanz, F. (2012). Multiple sclerosis risk variant HLA-DRB1*1501 associates with high expression of DRB1 gene in different human populations. PloS one, 7(1), e29819. https://doi.org/10.1371/journal.pone.0029819

24. Moutsianas, L., Jostins, L., Beecham, A. H., Dilthey, A. T., Xifara, D. K., Ban, M., Shah, T. S., Patsopoulos, N. A., Alfredsson, L., Anderson, C. A., Attfield, K. E., Baranzini, S. E., Barrett, J., Binder, T. M. C., Booth, D., Buck, D., Celius, E. G., Cotsapas, C., D'Alfonso, S., Dendrou, C. A., … McVean, G. (2015). Class II HLA interactions modulate genetic risk for multiple sclerosis. Nature genetics, 47(10), 1107–1113. https://doi.org/10.1038/ng.3395

25. International Multiple Sclerosis Genetics Consortium (2019). Multiple sclerosis genomic map implicates peripheral immune cells and microglia in susceptibility. Science (New York, N.Y.), 365(6460), eaav7188. https://doi.org/10.1126/science.aav7188

26. Ma, Q., Shams, H., Didonna, A., Baranzini, S. E., Cree, B. A. C., Hauser, S. L., Henry, R. G., & Oksenberg, J. R. (2023). Integration of epigenetic and genetic profiles identifies multiple sclerosis disease-critical cell types and genes. Communications Biology, 6(1). https://doi.org/10.1038/s42003-023-04713-5

27. Li, H., Hu, F., Zhang, Y., & Li, K. (2020). Comparative efficacy and acceptability of disease-modifying therapies in patients with relapsing–remitting multiple sclerosis: a systematic review and network meta-analysis. Journal of Neurology, 267(12), 3489-3498. https://doi.org/10.1007/s00415-019-09395-w

28. Kieseier B. C. (2011). The mechanism of action of interferon-β in relapsing multiple sclerosis. CNS drugs, 25(6), 491–502. https://doi.org/10.2165/11591110-000000000-00000

29. Namdar, A., Nikbin, B., Ghabaee, M., Bayati, A., & Izad, M. (2010). Effect of IFN-beta therapy on the frequency and function of CD4(+)CD25(+) regulatory T cells and Foxp3 gene expression in relapsing-remitting multiple sclerosis (RRMS): a preliminary study. J Neuroimmunol, 218(1-2), 120-124. https://doi.org/10.1016/j.jneuroim.2009.10.013

30. Kasindi, A., Fuchs, D. T., Koronyo, Y., Rentsendorj, A., Black, K. L., & Koronyo-Hamaoui, M. (2022). Glatiramer Acetate Immunomodulation: Evidence of Neuroprotection and Cognitive Preservation. Cells, 11(9), 1578. https://doi.org/10.3390/cells11091578

31. Häusler, D., Hajiyeva, Z., Traub, J. W., Zamvil, S. S., Lalive, P. H., Brück, W., & Weber, M. S. (2020). Glatiramer acetate immune modulates B-cell antigen presentation in treatment of MS. Neurology - Neuroimmunology Neuroinflammation, 7(3), e698. https://doi.org/10.1212/nxi.0000000000000698

32. Amin, M., & Hersh, C. M. (2023). Updates and advances in multiple sclerosis neurotherapeutics. Neurodegenerative disease management, 13(1), 47–70. https://doi.org/10.2217/nmt-2021-0058

33. Montalban, X., Hauser, S. L., Kappos, L., Arnold, D. L., Bar-Or, A., Comi, G., de Seze, J., Giovannoni, G., Hartung, H. P., Hemmer, B., Lublin, F., Rammohan, K. W., Selmaj, K., Traboulsee, A., Sauter, A., Masterman, D., Fontoura, P., Belachew, S., Garren, H., Mairon, N., … ORATORIO Clinical Investigators (2017). Ocrelizumab versus Placebo in Primary Progressive Multiple Sclerosis. The New England journal of medicine, 376(3), 209–220. https://doi.org/10.1056/NEJMoa1606468

34. Hofstetter, H. H., Shive, C. L., & Forsthuber, T. G. (2002). Pertussis toxin modulates the immune response to neuroantigens injected in incomplete Freund's adjuvant: induction of Th1 cells and experimental autoimmune encephalomyelitis in the presence of high frequencies of Th2 cells. J Immunol, 169(1), 117-125. https://doi.org/10.4049/jimmunol.169.1.117

35. Harkiolaki, M., Holmes, S. L., Svendsen, P., Gregersen, J. W., Jensen, L. T., McMahon, R., Friese, M. A., Van Boxel, G., Etzensperger, R., Tzartos, J. S., Kranc, K., Sainsbury, S., Harlos, K., Mellins, E. D., Palace, J., Esiri, M. M., Van Der Merwe, P. A., Jones, E. Y., & Fugger, L. (2009). T Cell-Mediated Autoimmune Disease Due to Low-Affinity Crossreactivity to Common Microbial Peptides. Immunity, 30(3), 348-357. https://doi.org/10.1016/j.immuni.2009.01.009

36. Spear, E. T., Holt, E. A., Joyce, E. J., Haag, M. M., Mawe, S. M., Hennig, G. W., Lavoie, B., Applebee, A. M., Teuscher, C., & Mawe, G. M. (2018). Altered gastrointestinal motility involving autoantibodies in the experimental autoimmune encephalomyelitis model of multiple sclerosis. Neurogastroenterol Motil, 30(9), e13349. https://doi.org/10.1111/nmo.13349

37. Chu, F., Shi, M., Zheng, C., Shen, D., Zhu, J., Zheng, X., & Cui, L. (2018). The roles of macrophages and microglia in multiple sclerosis and experimental autoimmune encephalomyelitis. J Neuroimmunol, 318, 1-7. https://doi.org/10.1016/j.jneuroim.2018.02.015

38. Clarkson, B. D., Walker, A., Harris, M., Rayasam, A., Sandor, M., & Fabry, Z. (2014). Mapping the accumulation of co-infiltrating CNS dendritic cells and encephalitogenic T cells during EAE. Journal of Neuroimmunology, 277(1-2), 39-49. https://doi.org/10.1016/j.jneuroim.2014.09.016

39. Pierson, E. R., Wagner, C. A., & Goverman, J. M. (2018). The contribution of neutrophils to CNS autoimmunity. Clin Immunol, 189, 23-28. https://doi.org/10.1016/j.clim.2016.06.017

40. Aubé, B., Lévesque, S. A., Paré, A., Chamma, É., Kébir, H., Gorina, R., Lécuyer, M. A., Alvarez, J. I., De Koninck, Y., Engelhardt, B., Prat, A., Côté, D., & Lacroix, S. (2014). Neutrophils mediate blood-spinal cord barrier disruption in demyelinating neuroinflammatory diseases. J Immunol, 193(5), 2438-2454. https://doi.org/10.4049/jimmunol.1400401

41. Sunnemark, D., Eltayeb, S., Nilsson, M., Wallström, E., Lassmann, H., Olsson, T., Berg, A.-L., & Ericsson-Dahlstrand, A. (2005). CX3CL1 (fractalkine) and CX3CR1 expression in myelin oligodendrocyte glycoprotein-induced experimental autoimmune encephalomyelitis: kinetics and cellular origin. Journal of Neuroinflammation, 2(1), 17. https://doi.org/10.1186/1742-2094-2-17

42. Hwang, D., Seyedsadr, M. S., Ishikawa, L. L. W., Boehm, A., Sahin, Z., Casella, G., Jang, S., Gonzalez, M. V., Garifallou, J. P., Hakonarson, H., Zhang, W., Xiao, D., Rostami, A., Zhang, G.-X., & Ciric, B. (2022). CSF-1 maintains pathogenic but not homeostatic myeloid cells in the central nervous system during autoimmune neuroinflammation. Proceedings of the National Academy of Sciences, 119(14). https://doi.org/10.1073/pnas.2111804119

43. Garcia, J. A., Pino, P. A., Mizutani, M., Cardona, S. M., Charo, I. F., Ransohoff, R. M., Forsthuber, T. G., & Cardona, A. E. (2013). Regulation of adaptive immunity by the fractalkine receptor during autoimmune inflammation. J Immunol, 191(3), 1063-1072. https://doi.org/10.4049/jimmunol.1300040

44. Eltayeb, S., Berg, A. L., Lassmann, H., Wallström, E., Nilsson, M., Olsson, T., Ericsson-Dahlstrand, A., & Sunnemark, D. (2007). Temporal expression and cellular origin of CC chemokine receptors CCR1, CCR2 and CCR5 in the central nervous system: insight into mechanisms of MOG-induced EAE. J Neuroinflammation, 4, 14. https://doi.org/10.1186/1742-2094-4-14

45. Huang, D. R., Wang, J., Kivisakk, P., Rollins, B. J., & Ransohoff, R. M. (2001). Absence of monocyte chemoattractant protein 1 in mice leads to decreased local macrophage recruitment and antigen-specific T helper cell type 1 immune response in experimental autoimmune encephalomyelitis. J Exp Med, 193(6), 713-726. https://doi.org/10.1084/jem.193.6.713

46. Drohomyrecky, P. C., Doroshenko, E. R., Akkermann, R., Moshkova, M., Yi, T. J., Zhao, F. L., Ahn, J. J., McGaha, T. L., Pahan, K., & Dunn, S. E. (2019). Peroxisome Proliferator–Activated Receptor-δ Acts within Peripheral Myeloid Cells to Limit Th Cell Priming during Experimental Autoimmune Encephalomyelitis. The Journal of Immunology, 203(10), 2588-2601. https://doi.org/10.4049/jimmunol.1801200

47. Pöllinger, B., Krishnamoorthy, G., Berer, K., Lassmann, H., Bösl, M. R., Dunn, R., Domingues, H. S., Holz, A., Kurschus, F. C., & Wekerle, H. (2009). Spontaneous relapsing-remitting EAE in the SJL/J mouse: MOG-reactive transgenic T cells recruit endogenous MOG-specific B cells. Journal of Experimental Medicine, 206(6), 1303-1316. https://doi.org/10.1084/jem.20090299

48. Aharoni, R., Eilam, R., Stock, A., Vainshtein, A., Shezen, E., Gal, H., Friedman, N., & Arnon, R. (2010). Glatiramer acetate reduces Th-17 inflammation and induces regulatory T-cells in the CNS of mice with relapsing-remitting or chronic EAE. J Neuroimmunol, 225(1-2), 100-111. https://doi.org/10.1016/j.jneuroim.2010.04.022

49. McGinley, A. M., Sutton, C. E., Edwards, S. C., Leane, C. M., Decourcey, J., Teijeiro, A., Hamilton, J. A., Boon, L., Djouder, N., & Mills, K. H. G. (2020). Interleukin-17A Serves a Priming Role in Autoimmunity by Recruiting IL-1β-Producing Myeloid Cells that Promote Pathogenic T Cells. Immunity, 52(2), 342-356.e346. https://doi.org/10.1016/j.immuni.2020.01.002

50. Tanwar, S., Oguz, C., Metidji, A., Dahlstrom, E., Barbian, K., Kanakabandi, K., Sykora, L., & Shevach, E. M. (2020). Type I IFN signaling in T regulatory cells modulates chemokine production and myeloid derived suppressor cells trafficking during EAE. J Autoimmun, 115, 102525. https://doi.org/10.1016/j.jaut.2020.102525

51. Luz-Crawford, P., Kurte, M., Bravo-Alegría, J., Contreras, R., Nova-Lamperti, E., Tejedor, G., Noël, D., Jorgensen, C., Figueroa, F., Djouad, F., & Carrión, F.

(2013). Mesenchymal stem cells generate a CD4+CD25+Foxp3+ regulatory T cell population during the differentiation process of Th1 and Th17 cells. Stem Cell Research & Therapy, 4(3), 65. https://doi.org/10.1186/scrt216

52. Alissafi, T., Kalafati, L., Lazari, M., Filia, A., Kloukina, I., Manifava, M., Lim, J.-H., Alexaki, V. I., Ktistakis, N. T., Doskas, T., Garinis, G. A., Chavakis, T., Boumpas, D. T., & Verginis, P. (2020). Mitochondrial Oxidative Damage Underlies Regulatory T Cell Defects in Autoimmunity. Cell Metabolism, 32(4), 591-604.e597. https://doi.org/10.1016/j.cmet.2020.07.001

53. Rangachari, M., & Kuchroo, V. K. (2013). Using EAE to better understand principles of immune function and autoimmune pathology. Journal of Autoimmunity, 45, 31-39. https://doi.org/10.1016/j.jaut.2013.06.008

54. Berard, J. L., Wolak, K., Fournier, S., & David, S. (2010). Characterization of relapsing-remitting and chronic forms of experimental autoimmune encephalomyelitis in C57BL/6 mice. Glia, 58(4), 434–445. https://doi.org/10.1002/glia.20935

55. Ashbrook, D. G., Arends, D., Prins, P., Mulligan, M. K., Roy, S., Williams, E. G., Lutz, C. M., Valenzuela, A., Bohl, C. J., Ingels, J. F., McCarty, M. S., Centeno, A. G., Hager, R., Auwerx, J., Lu, L., & Williams, R. W. (2021). A platform for experimental precision medicine: The extended BXD mouse family. Cell Systems, 12(3), 235-247.e239. https://doi.org/10.1016/j.cels.2020.12.002

56. Wang, J., Yoon, T. W., Read, R., Yi, A. K., Williams, R. W., & Fitzpatrick, E. A. (2020). Genetic variability of T cell responses in hypersensitivity pneumonitis identified using the BXD genetic reference panel. American journal of physiology. Lung cellular and molecular physiology, 318(4), L631–L643. https://doi.org/10.1152/ajplung.00120.2019

57. Maatta, Nygardas, & Hinkkanen. (2000). Enhancement of Experimental Autoimmune Encephalomyelitis Severity by Ultrasound Emulsification of Antigen/Adjuvant in Distinct Strains of Mice. Scandinavian Journal of Immunology, 51(1), 87-90. https://doi.org/10.1046/j.1365-3083.2000.00686.x

58. Alam, M. S., Otsuka, S., Wong, N., Abbasi, A., Gaida, M. M., Fan, Y., Meerzaman, D., & Ashwell, J. D. (2021). TNF plays a crucial role in inflammation by signaling via T cell TNFR2. Proceedings of the National Academy of Sciences of the United States of America, 118(50), e2109972118. https://doi.org/10.1073/pnas.2109972118

59. Ponzone, A., Spada, M., Ferraris, S., Dianzani, I., & de Sanctis, L. (2004). Dihydropteridine reductase deficiency in man: from biology to treatment. Medicinal research reviews, 24(2), 127–150. https://doi.org/10.1002/med.10055

60. Kirsty, C. W., Mary, H., & Sumner, J. (2022). The Relationship of Cobalamin and/or Folate to the Patient-Centred Outcomes in Multiple Sclerosis: A Systematic Review and Meta-analysis. Nutrition and health, 28(4), 527–542. https://doi.org/10.1177/02601060221080240

61. Preston, S. P., Doerflinger, M., Scott, H. W., Allison, C. C., Horton, M., Cooney, J., & Pellegrini, M. (2021). The role of MKK4 in T-cell development and immunity to viral infections. Immunology and cell biology, 99(4), 428–435. https://doi.org/10.1111/imcb.12426

62. Oltmanns, U., Issa, R., Sukkar, M. B., John, M., & Chung, K. F. (2003). Role of c-jun N-terminal kinase in the induced release of GM-CSF, RANTES and IL-8 from human airway smooth muscle cells. British journal of pharmacology, 139(6), 1228–1234. https://doi.org/10.1038/sj.bjp.0705345

63. Ajami, B., Bennett, J. L., Krieger, C., McNagny, K. M., & Rossi, F. M. (2011). Infiltrating monocytes trigger EAE progression, but do not contribute to the resident microglia pool. *Nature neuroscience*, *14*(9), 1142–1149. https://doi.org/10.1038/nn.2887

64. Hofstetter, H. H., Shive, C. L., & Forsthuber, T. G. (2002). Pertussis toxin modulates the immune response to neuroantigens injected in incomplete Freund's adjuvant: induction of Th1 cells and experimental autoimmune encephalomyelitis in the presence of high frequencies of Th2 cells. Journal of immunology (Baltimore, Md. : 1950), 169(1), 117–125. https://doi.org/10.4049/jimmunol.169.1.117

65. Krishnarajah, S., & Becher, B. (2022). TH Cells and Cytokines in Encephalitogenic Disorders. Frontiers in immunology, 13, 822919. https://doi.org/10.3389/fimmu.2022.822919

66. Axtell, R. C., de Jong, B. A., Boniface, K., van der Voort, L. F., Bhat, R., De Sarno, P., Naves, R., Han, M., Zhong, F., Castellanos, J. G., Mair, R., Christakos, A., Kolkowitz, I., Katz, L., Killestein, J., Polman, C. H., de Waal Malefyt, R., Steinman, L., & Raman, C. (2010). T helper type 1 and 17 cells determine efficacy of interferon-beta in multiple sclerosis and experimental encephalomyelitis. Nature medicine, 16(4), 406–412. https://doi.org/10.1038/nm.2110

67. Koutrolos, M., Berer, K., Kawakami, N., Wekerle, H., & Krishnamoorthy, G. (2014). Treg cells mediate recovery from EAE by controlling effector T cell proliferation and motility in the CNS. Acta neuropathologica communications, 2, 163. https://doi.org/10.1186/s40478-014-0163-1

68. Wang, C., Zhou, W., Su, G., Hu, J., & Yang, P. (2022). Progranulin Suppressed Autoimmune Uveitis and Autoimmune Neuroinflammation by Inhibiting Th1/Th17 Cells and Promoting Treg Cells and M2 Macrophages. Neurology(R)

neuroimmunology & neuroinflammation, 9(2), e1133. https://doi.org/10.1212/NXI.0000000000001133

69. Bar-Or, A., & Li, R. (2021). Cellular immunology of relapsing multiple sclerosis: interactions, checks, and balances. Lancet Neurol, 20(6), 470-483. https://doi.org/10.1016/s1474-4422(21)00063-6

70. Dhaiban, S., Al-Ani, M., Elemam, N. M., & Maghazachi, A. A. (2020). Targeting Chemokines and Chemokine Receptors in Multiple Sclerosis and Experimental Autoimmune Encephalomyelitis. Journal of inflammation research, 13, 619–633. https://doi.org/10.2147/JIR.S270872

71. Muzio, L., Cavasinni, F., Marinaro, C., Bergamaschi, A., Bergami, A., Porcheri, C., Cerri, F., Dina, G., Quattrini, A., Comi, G., Furlan, R., & Martino, G. (2010). Cxcl10 enhances blood cells migration in the sub-ventricular zone of mice affected by experimental autoimmune encephalomyelitis. Molecular and cellular neurosciences, 43(3), 268–280. https://doi.org/10.1016/j.mcn.2009.11.008

72. Krensky, A. M., & Ahn, Y. T. (2007). Mechanisms of disease: regulation of RANTES (CCL5) in renal disease. Nature clinical practice. Nephrology, 3(3), 164–170. https://doi.org/10.1038/ncpneph0418

73. Tang, S., Su, B., Tao, T., Yan, W., Zhang, R., Qin, X., & Feng, J. (2022). RGMa regulates CCL5 expression via the BMP receptor in experimental autoimmune encephalomyelitis mice and endothelial cells. Molecular medicine reports, 25(3), 85. https://doi.org/10.3892/mmr.2022.12601

74. Alam, M. S., Otsuka, S., Wong, N., Abbasi, A., Gaida, M. M., Fan, Y., Meerzaman, D., & Ashwell, J. D. (2012). TNF plays a crucial role in inflammation by signaling via T cell TNFR2. Proceedings of the National Academy of Sciences of the United States of America, 118(50), e2109972118. https://doi.org/10.1073/pnas.2109972118

VITA

Margaret Caroline Danehy was born in 1996 in Memphis, TN to Jennifer and Patrick Danehy. She attended high school at Lausanne Collegiate School and graduated in 2014. She attended Elon University and graduated in 2018, receiving her Bachelor of Science in Biology in the Molecular and Cellular Biology tract. She then worked as a Laboratory Technician at St. Jude Children's Research Hospital for two years. In 2020, she began the Integrated Biomedical Sciences program at the University of Tennessee Health Science Center and joined Dr. Fitzpatrick's lab in 2021. She hopes to graduate from the College of Graduate Health Sciences with a master's in science degree from the Biomedical Sciences program, with a concentration in Microbiology, Immunology, and Biochemistry in December 2023.